

Cite this: DOI: 10.1039/c0dt01599g

www.rsc.org/dalton

PERSPECTIVE

Radiometallated peptides for molecular imaging and targeted therapy

João D. G. Correia, António Paulo, Paula D. Raposinho and Isabel Santos*

Received 17th November 2010, Accepted 11th January 2011

DOI: 10.1039/c0dt01599g

In developed countries, cancer is the second leading cause of death, being only surpassed by cardiovascular diseases. To develop tumor-targeted tools to localize and treat cancer at an early stage is a multidisciplinary area fuelled by the convergence of biology, medicine, chemistry, physics and engineering. Chemists, in particular, play a critical role in this effort, as they are continuously challenged to use innovative chemical strategies to develop 'smart drugs'. The *in vitro* observation that peptide receptors are overexpressed in certain tumors, as compared to endogenous expression levels, has prompted the use of such receptors as targets and the design of radiolabelled peptide-based tools for targeted nuclear molecular imaging and therapy. Such approach has gained increased interest over the last two decades, driven in particular by the success of OctreoScan[®] and by the increasing knowledge concerning overexpression of regulatory peptide receptors in tumor tissues. Selected peptides that target a variety of disease related receptors are in place and have been labeled with different radiometals, using mainly the bifunctional approach. This review begins by summarizing some relevant aspects of the coordination chemistry of the metals studied for labeling peptides. Then, we provide an overview of the chemical strategies explored to improve the biological performance of different families of radiometallated peptides for nuclear molecular imaging and/or targeted radionuclide tumor therapy.

Introduction

Despite the advances in medical sciences, cancer is still a leading cause of death worldwide. The World Health Organization reported that, in developed countries, cancer is the second leading cause of death, being only surpassed by cardiovascular diseases.¹ Nevertheless, during recent decades, remarkable insights into the cell and molecular biology of malignancies has been acquired, and a myriad of differences in the biological make-up of cancers compared with their healthy-tissue counterparts have been catalogued.²⁻⁴ The increasing knowledge generated by such achievements has led to the identification of several biomarkers, and some of them have been considered as potential targets for *in vivo* molecular imaging and/or therapeutic purposes.^{2,3,5-7} Among others, antigens, membrane receptors and enzymes have been considered as interesting biomarkers, since they play important roles in pathological processes, being in most cases overexpressed or upregulated compared to endogenous expression levels. The validation and potential interest of those targets have been intensively studied, and the identification and design of high-affinity binders for such targets has been – and remains – an area of intense research. The optimization of endogenous ligands has been the most widely used strategy to generate high-affinity ligands.^{2,3,5-7}

Nuclear medicine uses radiolabelled compounds for *in vivo* imaging and therapeutic purposes. Such compounds are named radiopharmaceuticals and are used in such low concentrations that they have no pharmacological effect. When specific, radiopharmaceuticals consist of a target-specific moiety, such as an antibody or antibody fragment, peptides or low molecular weight ligands, linked to an appropriate radionuclide. Depending on the intrinsic physical characteristics of the radionuclide, the radiopharmaceuticals are used for *in vivo* imaging or targeted-radionuclide therapy (TRT). Single-photon emission computed tomography (SPECT) and positron emission tomography (PET) are the two imaging modalities used in nuclear medicine. These modalities are able to determine the concentration of specific molecules in the human body in a non-invasive way, and are sensitive enough to visualize interactions between physiological targets and ligands.^{3,5-7} TRT involves specific localization of a radionuclide emitting ionizing radiation to deliver a cytotoxic radiation dose to cancerous tissues, while sparing the surrounding healthy ones.^{6,8,9}

Table 1 summarizes the most relevant radionuclides with medical interest in nuclear medicine, for both diagnostic (γ or β^+ emitters) and therapeutic applications (β^- , α or Auger electron emitters).

In terms of target-specific moieties, monoclonal antibodies have long been considered interesting biomolecules for cancer diagnosis and therapy, and represent the start of a new era in cancer management.⁸⁻¹⁰ Owing to some drawbacks, namely poor pharmacokinetics, some improvements through protein

Unidade de Ciências Químicas e Radiofarmacêuticas, Instituto Tecnológico e Nuclear, Estrada Nacional 10, Sacavém, 2686-953, Portugal. E-mail: isantos@itn.pt; Fax: +351 21-9946185; Tel: +351 21-9946201

Table 1 Relevant radionuclides for medical applications

Nuclide	Physical half-life	Mode of decay (%)	Application
^{99m} Tc	6.0 h	IT (100)	SPECT
¹⁸⁶ Re	89.2 h	β ⁻ (92) EC (8)	Therapy
¹⁸⁸ Re	17 h	β ⁻ (100)	Therapy
¹²³ I	13.2 h	EC (100)	SPECT
¹³¹ I	8.02 d	β ⁻ (100)	Therapy
¹⁸ F	109.8 min	β ⁺ (97) EC (3)	PET
¹¹ C	20.3 min	β ⁺ (100)	PET
⁸⁶ Y	14.7 h	β ⁺ (33) EC (66)	PET
⁹⁰ Y	64.1 h	β ⁻ (100)	Therapy
¹¹¹ In	2.80 d	EC (100)	SPECT
⁶⁷ Ga	3.26 d	EC (100)	SPECT
⁶⁸ Ga	67.8 min	β ⁺ (99) EC (10)	PET
⁶⁰ Cu	0.4 h	β ⁺ (93) EC (7)	PET
⁶¹ Cu	3.3 h	β ⁺ (62) EC (38)	PET
⁶² Cu	0.16 h	β ⁺ (98) EC (2)	PET
⁶⁴ Cu	12.7 h	β ⁻ (40), β ⁺ (19) EC (41)	PET/Therapy
⁶⁷ Cu	61.8 h	β ⁻ (100)	Therapy
⁸⁹ Zr	78.5 h	β ⁺ (22.7) EC (77)	PET
¹⁵³ Sm	46.3 d	β ⁻ (100)	Therapy
¹⁶⁶ Ho	26.8 d	β ⁻ (100)	Therapy
¹⁷⁷ Lu	6.73 d	β ⁻ (100)	Therapy

engineering have been made in the last few years, and the dream of targeted radionuclide therapy was partially fulfilled with the introduction of radiolabelled antibodies for clinical use, such as Zevalin (murine antibody-⁹⁰Y) and Bexxar (murine antibody-¹³¹I). Despite these successful examples, there is still room for improvement, and attempts to find targeted radionuclide therapy for solid tumors^{8–10} makes this a very active research area.

Following the finding that small regulatory peptide receptors are often overexpressed in certain human cancers and that derivatives of their natural ligands can be used for tumor targeting, the use of peptides has appeared as another approach for delivering radioactivity to tumors. This approach has gained increased interest over the last two decades, driven in particular by the success of OctreoScan® (¹¹¹In-labelled somatostatin analog) in the late 1980s and by the increasing knowledge concerning overexpression of regulatory peptide receptors in tumor tissues.^{2,3,5–7,11} The availability of different techniques to generate potential high-affinity peptides for a selected target is also responsible for the large pool of bioactive synthetic peptides. Indeed, target-specific delivery of radioactive peptides, both for molecular imaging and therapy, is increasingly considered a promising strategy. Well-established solid-phase peptide synthesis allows reproducible preparation of a variety of peptides with accurate chemical structures, which can be modulated to optimize affinity and specificity for the target, metabolic stability and pharmacokinetics.

Most of the naturally occurring peptides have a short biological half-life due to rapid degradation by various peptidases and proteases found in plasma. Once the biological portion of the peptides has been identified, they can be engineered to prolong their biological half-lives *in vivo*. Such improvement can be

done by the introduction of D-amino acids, incorporation of amino alcohol, use of unusual amino acids or side-chains and amidation and/or acetylation of peptide C- and N-termini. The pharmacokinetics of peptides can also be tuned by altering the hydrophilic and hydrophobic balance of the peptide structure, through the introduction of charged amino acids (e.g. glutamic acid), carbohydrates or poly(ethylene)glycol (PEG) chains in the peptide backbone.

Another advantage of peptides is their tolerance towards the modifications necessary for their labeling with different radionuclides. For radiometallation, for example, the most explored approach makes use of a bifunctional chelator (BFC) that coordinates the metal and presents an adequate functionality for the coupling of the targeting peptide. Additionally, an appropriate linker that separates the chelating moiety and the bioactive fragment can also be used. The nature of such linkers is variable, and generally they are also used as pharmacokinetic modifiers.

However, it must be kept in mind that the design of a peptide-based radiopharmaceutical is a non-trivial task, due to the relatively small size of the targeting peptide. All the structural modifications have to be done with retention of its affinity and selectivity to the putative receptors. Moreover, the radiolabeled peptide must be obtained with high specific activity, show a high stability under physiological conditions, and present high selectivity and target-specific uptake, with low accumulation in non-target tissues.

Herein, we will present an overview of the chemical efforts made to find metallated peptides for nuclear molecular imaging and TRT. In the first section, we will present relevant aspects of the coordination chemistry of metals with medical interest in nuclear medicine, for both diagnostic and therapeutic applications. The second section will present a broad view of the chemical strategies explored to synthesize different families of radiometallated peptides, as well as the chemical efforts made to improve their biological performance. This contribution intends to update previous reviews, but will not cover work on radiolabeled somatostatin analogs for imaging or therapy of tumors, since these radiopeptides have been the focus of various comprehensive reviews recently published.^{12–17} To provide some context to the current manuscript, some overlap with earlier reviews is unavoidable.^{18,19}

Relevant coordination chemistry

Acyclic and cyclic polyaminopolycarboxylic ligands (Fig. 1), such as diethylenetriaminepentacetic acid (DTPA), 1,4,7,10-tetraazacyclododecane-1,4,7,10-tetraacetic acid (DOTA), 1,4,8,11-tetraazacyclododecane-1,4,8,11-tetraacetic acid (TETA), 1,4,7-triazacyclononane-1,4,7-triacetic acid (NOTA) and cross-bridged (CB) tetraazamacrocyclic derivatives, have been the most extensively evaluated BFCs for the labeling of peptides with trivalent and bivalent radiometals like Ga³⁺, In³⁺, Y³⁺ and Ln³⁺ or Cu²⁺.^{20–23} One of the carboxylic arms of polyaminopolycarboxylic ligands can be used for the coupling of the peptide, typically *via* formation of amide bonds with primary amines from lysine residues or the N-terminus of peptides, without compromising the stability of the respective metal complexes.

Alternatively, the functional group used to couple the peptide can be introduced in the methylenic backbone of the chelator,

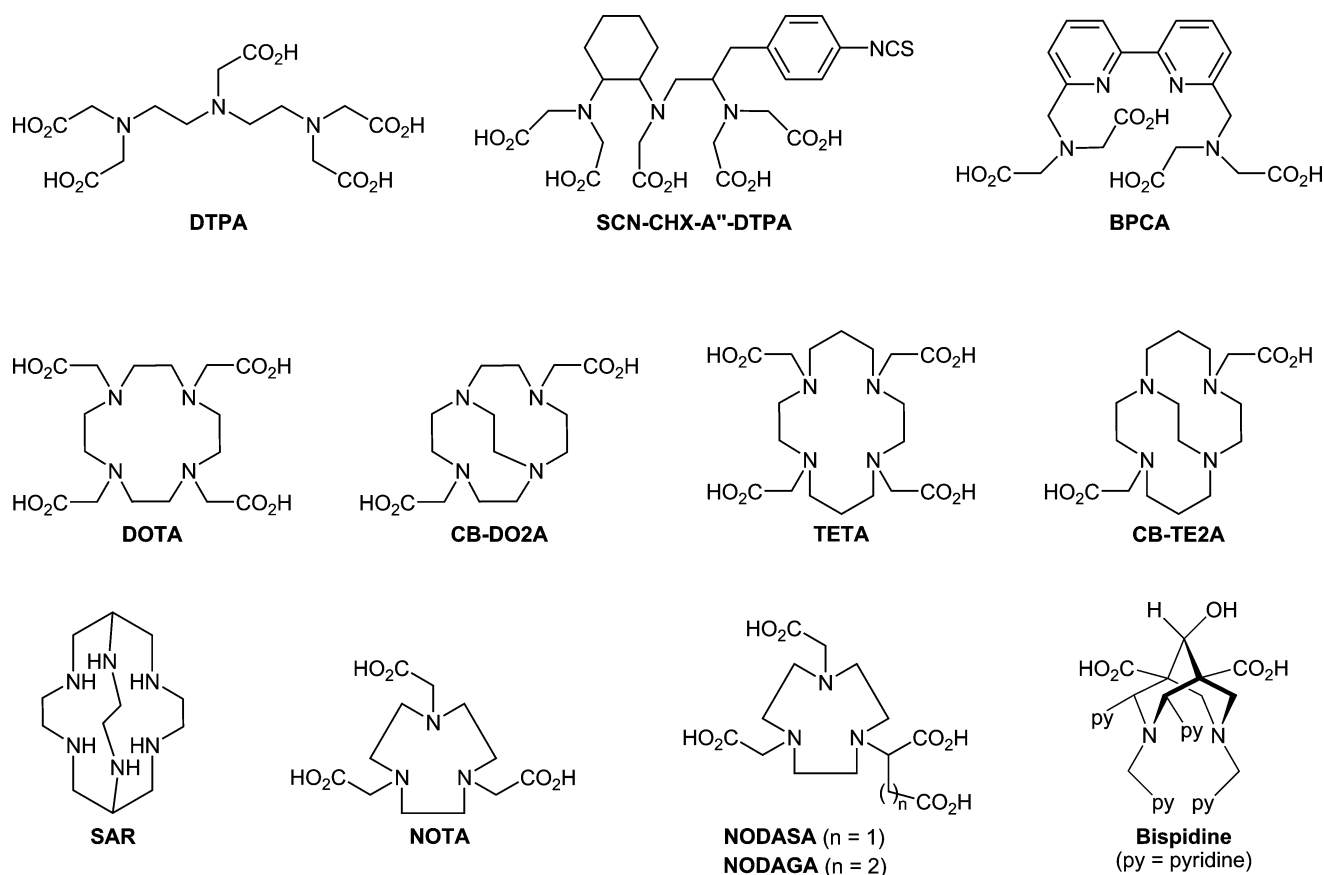


Fig. 1 Acyclic and cyclic polyaminocarboxylic ligands.

leaving all of the carboxylic pendant arms available for coordination to the metal. A variety of possibilities can be explored to couple the peptide to the chelator. If the coupling involves a carboxylic group from the chelator, it is possible to perform the activation of the carboxyl group *in situ* using the common activation strategies, like those based on the formation of tetrafluorophenyl or *N*-hydroxysuccinimide activated esters. Another alternative is the introduction of maleimide or isocyanate functions in the chelator framework, which promptly react with thiol or amino groups of the peptide with formation of thioether or thiourea bonds.^{24,25}

Macrocyclic chelators provide metal complexes that are thermodynamically more stable and kinetically more inert than the complexes with their acyclic counterparts, as a consequence of the ability of the free macrocycles to adopt preorganized conformations.²⁶ Table 2 summarizes the stability constants (K_{ML}) for complexes of some of the metals reviewed herein with the most common acyclic or macrocyclic polyaminopolycarboxylic ligands (Fig. 1). By themselves, these K_{ML} values can indicate the relative affinity of the different chelators for a given metal. However, one has to consider that it can be difficult to compare stability constants for ligands of different basicity. To overcome such difficulty, the respective pM values must be considered.

Among the several polyaminopolycarboxylic ligands, DOTA-like chelators do not always provide for the most stable complexes (Table 2). Nevertheless, so far, DOTA-like chelators have been extensively used for the radiometallation of peptides, most proba-

Table 2 Stability constants ($\log K_{ML}$) for complexes of polyaminocarboxylates with divalent and trivalent metal ions

Chelator	Metal				
	Cu(II)	Ga(III)	In(III)	Y(III)	Lu(III)
DTPA	21.5 ^b	25.5 ^b	29.5 ^h	22.5 ^j	—
DOTA	22.3 ^c	21.3 ^e	23.9 ^f	24.3 ^j	25.5 ^{l,m}
TETA	21.7 ^d	19.7 ^f	21.8 ^f	14.8 ^k	15.3 ^k
NOTA	21.63 ^e	31.0 ^f	26.2 ⁱ	—	—

^a $K_{ML} = [ML]/[M][L]$. ^b Ref. 27. ^c Ref. 28. ^d Ref. 29. ^e Ref. 30. ^f Ref. 31. ^g Ref. 32. ^h Ref. 33. ⁱ Ref. 34. ^j Ref. 35. ^k Ref. 36. ^l Ref. 37. ^m Ref. 38.

bly due to the commercial availability of several activated DOTA derivatives ready for conjugation.

Gallium and indium

The group 13 elements gallium (Ga) and indium (In) are post-transition metals presenting radionuclides suitable for SPECT (⁶⁷Ga, ¹¹¹In) and PET (⁶⁸Ga) imaging, or for Auger-therapy (¹¹¹In) (Table 1). ⁶⁷Ga and ¹¹¹In are cyclotron-produced gamma emitters obtained at reasonable cost and are deliverable to different users over relatively large distances. ⁶⁸Ga is a positron emitter readily accessible from the ⁶⁸Ge/⁶⁸Ga generator, offering the possibility to obtain on site a PET radionuclide without needing the presence of a nearby cyclotron.^{23,39}

The chemistry of gallium and indium in aqueous media is exclusively limited to the oxidation state III. In aqueous solution, the M^{3+} ($M = \text{Ga}, \text{In}$) ions have a marked tendency to undergo hydrolysis, which is even more pronounced for Ga(III). At physiological pH, gallium forms essentially the soluble gallate anion $[\text{Ga}(\text{OH})_4]^-$, while indium precipitates as the tris(hydroxide) $[\text{In}(\text{OH})_3]$. When designing radiopharmaceuticals, namely radiometallated peptides, it is of particular importance to obtain Ga and In complexes resistant to hydrolysis. These complexes must also have resistance towards transchelation reactions with transferrin, which is a protein present in the plasma and involved in the receptor-mediated transport of iron into cells. This is particularly relevant for Ga(III), that presents the highest affinity to transferrin due to the similarity of the coordination chemistry of trivalent gallium and iron.^{40,41}

Both Ga(III) and In(III) are rather hard Lewis acids and, for this reason, the formation of stable complexes with these metal ions usually requires the use of polydentate chelators presenting anionic oxygen donor groups, such as acyclic or macrocyclic polyaminocarboxylic ligands (Fig. 1). The difference on the ionic radius of Ga^{3+} (47–62 pm, CN = 4–6) and In^{3+} (62–92 pm, CN = 4–8) is another important aspect to take into consideration when selecting a proper ligand for labeling a biomolecule with their radioisotope. The maximum coordination number (CN) attained by Ga(III) complexes is 6 while In(III), being larger, forms complexes with CN = 7 and even with CN = 8. These differences are well documented by several X-ray structures of Ga(III) and In(III) complexes with polyaminocarboxylic ligands, as exemplified in Fig. 2 for a DOTA derivative containing a pendant arm functionalized with a triphenylphosphonium (TPP) group. The Ga(III) complex is hexacoordinated with a distorted octahedral geometry, and the In(III) complex is heptacoordinated with a monocapped trigonal prismatic geometry.⁴²

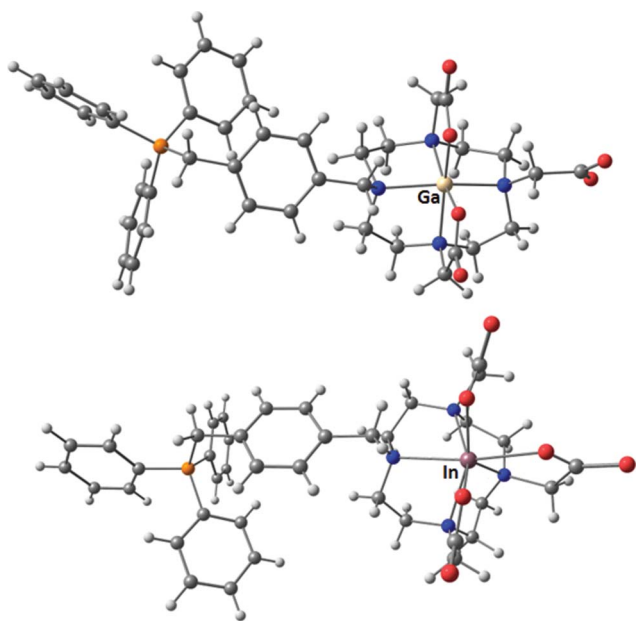


Fig. 2 Molecular structures of Ga-DOTA-TPP and In-DOTA-TPP.⁴²

The labeling of peptides with $^{67}\text{Ga}/^{68}\text{Ga}$ has been performed using mainly DOTA or NOTA derivatives as bifunctional chela-

tors, while DTPA and DOTA derivatives have been used for ^{111}In -labeling of peptides. DTPA is potentially octadentate and forms complexes of higher stability with In(III) compared to Ga(III) (Table 2).

The Ga(III)-NOTA complex has an exquisite stability among gallium complexes, presenting a thermodynamic stability ($\log K = 31.0$, $\text{pM} = 26.4$) approximately 10 orders of magnitude higher than the one of Ga(III)-DOTA ($\log K = 21.3$, $\text{pM} = 15.2$). Moreover, the kinetics of complexation of Ga(III) is faster for NOTA than for DOTA, necessitating longer reaction times and higher temperatures to label peptides with $^{67/68}\text{Ga}$ using DOTA-like chelators. For this reason, NOTA-like chelators are very favorable for $^{67/68}\text{Ga}$ labeling of peptides. The high stability constant of Ga(III)-NOTA complexes and their kinetics certainly reflect a better fitting of the NOTA cavity size with the size of the Ga^{3+} ion and the involvement of all pendant arms in the coordination to the metal. To keep the possibility of a N_3O_3 -hexadentate coordination after linkage of the biomolecule, NOTA-like chelators containing a diacid pendant arm, such as NODASA (1,4,7-triazacyclononane-*N*-succinic acid-*N',N''*-diacetic acid) and NODAGA ((1,4,7-triazacyclononane-*N*-glutamic acid-*N',N''*-diacetic acid), have been designed and synthesized (Fig. 1).^{43,44} Unlike Ga(III), the coordination requirements of In(III) are not fulfilled by NOTA-like chelators which, for this reason, are not the best suited bifunctional chelators for the labeling of peptides with ^{111}In .

Yttrium and the lanthanides

Yttrium (Y) and the lanthanides (Ln) are trivalent metals that offer differing β -emitting radioisotopes relevant for therapeutic applications. Among these radioisotopes, ^{90}Y and the radiolanthanide ^{177}Lu have been the most extensively explored to obtain radiometallated peptides for peptide receptor radionuclide therapy (PRRT).^{20,45,46}

The aqueous coordination chemistry of yttrium and lanthanides shows a great similitude due to their common tricationic charge and similar ionic radii. The Y^{3+} and Ln^{3+} metal ions show a hard acidic character and tend to form complexes with hard donor atom ligands, displaying high coordination numbers, usually 8 or 9. Therefore, the labeling of peptides with these radiometals has been performed using mainly polyaminocarboxylic ligands. Acyclic DTPA derivatives form by far more stable complexes with In(III) than with Y(III) or Ln(III) (Table 1). The latter metal ions are coordinated more avidly by DOTA derivatives, due to the higher thermodynamic stability and enhanced kinetic inertness of the corresponding complexes. These features explain why DOTA-like compounds can be considered as the best choice for labeling peptides with ^{90}Y or ^{177}Lu , although DTPA derivatives have been used in several instances for that purpose. The high stability of Y-DOTA and Lu-DOTA complexes can be accounted for by the good match of the DOTA cavity size to the ionic radii of these trivalent metal ions. A poor match between Y^{3+} and Lu^{3+} ions and the cavity size of TETA derivatives justifies the much lower stability of M-TETA complexes ($M = \text{Y}, \text{Lu}$). For this reason, TETA chelators are not a good option for ^{90}Y - or ^{177}Lu -labeling of peptides.

Even after functionalization of one pendant arm with a targeting biomolecule, it is considered that DOTA-like chelators act as N_4O_4 -octadentate donor ligands towards Ln^{3+} and Y^{3+} ions,

as the amide oxygen from the conjugating arm also coordinates to the metal. This coordination mode has been confirmed by X-ray structural analysis of the model compound Y-DOTA-DPheNH₂ that contains a DOTA derivative with a carboxymethyl arm functionalized with phenylalanine (Fig. 3).⁴⁷ NMR studies of a related yttrium complex bearing a *p*-aminoanilide (AA) functionalized pendant arm, Y-DOTA-AA, have shown the retention of the octadentate coordination of the DOTA derivative in solution.⁴² This macrocyclic ligand in the congener In-DOTA-AA is also octa-coordinated but the In(III) complex is fluxional in solution at room temperature, most probably due to de-coordination/coordination of the amide oxygen from the functionalized pendant arm.⁴⁸ Such differences can affect the *in vivo* behavior of congener In(III) and Y(III) complexes and, eventually, may explain the discrepancies observed for the biological performance of similar ⁹⁰Y or ¹¹¹In-DOTA-AA complexes. Despite such differences, in radiopharmaceutical chemistry ¹¹¹In complexes are often used as surrogates to estimate the biodistribution and radiation dosimetry of congener ⁹⁰Y complexes. However, such studies need to take into consideration the differences in solution of Y(III) and In(III) complexes.

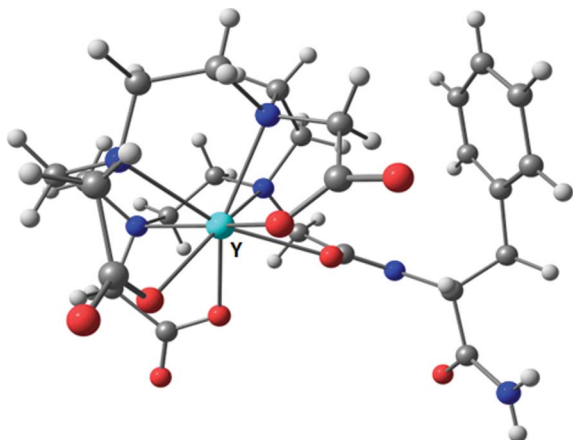


Fig. 3 Molecular structure of Y-DOTA-DPheNH₂.⁴⁷

Yttrium(III) and lanthanide(III) complexes of DOTA derivatives can exist in two interconverting diastereoisomers of square antiprism (SAP) and twisted square antiprism (TSAP) geometries. The ratio SAP/TSAP depends very much on the size of the trivalent ion being preferred the SAP geometry for the largest ions, like Y³⁺ or Lu³⁺. At macroscopic level, the formation and interconversion of these coordination isomers has been intensively studied by different research groups using NMR techniques.^{49,50} Studies on the formation of different coordination isomers of DOTA-like chelators using trivalent radiometals are scarce. Recently, it has been shown that a DOTA derivative ((*S*)-*p*-NH₂-Bn-DOTA) bearing a benzyl amine substituent at the methylenic backbone of the macrocycle forms a mixture of two isomers when labeled with ⁸⁶Y (β⁺ emitter; *t*_{1/2} = 14.7 h).⁵¹ As expected, the SAP isomer is predominant, being observed a SAP/TSAP ratio of 3 : 1. After separation by HPLC, the biodistribution profile of each isomer of [⁸⁶Y((*S*)-*p*-NH₂-Bn-DOTA)] was assessed using Wistar rats. Only minor differences were observed in their biological behavior, which may indicate that the isomerism of Y(III) complexes with DOTA-like chelators does not strongly influence their *in vivo* behavior.

Copper

Copper has a unique combination of diagnostic (⁶⁰Cu, ⁶¹Cu, ⁶²Cu and ⁶⁴Cu) and therapeutic radionuclides (⁶⁴/⁶⁷Cu) (Table 1). Moreover, due to its nuclear properties, ⁶⁴Cu is suitable for PET imaging and for TRT.^{21,23}

From the three accessible oxidation states (I–III) of copper under aqueous solution, Cu(II) has been the most widely used to obtain ⁶⁴Cu complexes potentially useful as radiopharmaceuticals. This reflects the fact that Cu(III) is relatively rare and difficult to stabilize in aqueous solution, while Cu(II) complexes display an increased kinetic inertness compared with Cu(I) complexes. To find labeling methodologies to prepare ⁶⁴Cu(II) complexes stable *in vivo*, it is necessary to take into consideration basic aspects of the aqueous coordination chemistry of Cu(II), as well as the behavior of copper as an essential trace metal in human biochemistry. The ⁶⁴Cu(II) complexes must be resistant towards transchelation to proteins involved in the transport and storage of copper, and must not undergo reduction to Cu(I), as it will increase the probability of releasing the radiometal *in vivo*.

DOTA and TETA have been largely used as bifunctional chelators for ⁶⁴Cu-labeling of peptides, although they are not ideal chelators for Cu(II), as well documented by the *in vivo* instability of their complexes. *In vivo* experiments in rat models have shown that both ⁶⁴Cu-DOTA and ⁶⁴Cu-TETA undergo transchelation of ⁶⁴Cu(II) to liver and blood proteins, with this behavior being more pronounced in the case of ⁶⁴Cu-DOTA.⁵² These macrocyclic complexes present a high thermodynamic stability with almost coincident *K*_{ML} values (Table 2), indicating that their kinetic inertness has a more crucial influence on their *in vivo* instability.

The 9-membered triazamacrocycle NOTA has also a good affinity for divalent copper, and the corresponding Cu(II)-NOTA complex presents a stability constant similar to those with DOTA and TETA (Table 2).^{53–56} NOTA-based bifunctional chelators allowed the ⁶⁴Cu-labeling of different bioactive peptides in very high specific activity and under mild reaction conditions. As reviewed below, the resulting metallopeptides have shown a better biodistribution profile than those labeled with ⁶⁴Cu using DOTA or TETA derivatives as BFCs, pointing out the best properties of NOTA-derivatives to stabilize the radiometal *in vivo*.⁵⁷

Different investigators have synthesized cross-bridged (CB) tetraazamacrocycles, aiming to introduce novel classes of bifunctional chelators suited for the *in vitro* and *in vivo* stabilization of Cu(II) complexes.^{20,23} The cyclen-based 4,10-bis(carboxymethyl)-1,4,7,10-tetraazabicyclo-[5.5.2]tetradecane (CB-DO2A) and the cyclam-based 4,11-bis(carboxymethyl)-1,4,8,11-tetraazabicyclo-[6.6.2]tetradecane (CB-TE2A) were used to prepare the complexes ⁶⁴Cu-CB-DO2A and ⁶⁴Cu-CB-TE2A. Metabolic studies in rat models showed that ⁶⁴Cu-CB-DO2A and ⁶⁴Cu-CB-TE2A presented an increased *in vivo* stability compared with ⁶⁴Cu-DOTA and ⁶⁴Cu-TETA complexes, confirming that the introduction of the ethylenic bridge enhances the stability of these macrocyclic Cu(II) complexes.^{52,58} In particular, the combination of the cyclam backbone with the cross-bridge significantly enhanced the *in vivo* stability of ⁶⁴Cu-CB-TE2A.

However, the kinetics of Cu(II) complexation by CB-TE2A is rather slow, and the formation of ⁶⁴Cu-CB-TE2A requires relatively harsh radiolabeling conditions that may induce damage to some biomolecules. Hence, there is still room for finding

bifunctional chelators that efficiently bind to Cu(II) under mild reaction conditions.

Looking to achieve such goals, cryptand macrocyclic ligands of the hexaaminemacrobicyclic type (Fig. 1), known as sarcophagines (Sar's), have been used as BFCs to label a few antibodies and peptides with ^{64}Cu .^{59–65} The Sar ligands encapsulate the Cu(II) ion, forming hexacoordinated and octahedral Cu(II) complexes with thermodynamic stability constants as high as the ones found with DOTA and TETA derivatives. At room temperature, the Sar ligands bind to ^{64}Cu (II) with fast complexation kinetics, at remarkably low concentrations over a pH range of 4–9. The resulting complexes show a high kinetic inertness, as shown by negligible *in vitro* transchelation.

Potentially hexadentate acyclic ligands of the bispidine type (Fig. 1) have been also envisaged as promising bifunctional chelators for ^{64}Cu -labeling of biomolecules, offering different positions of the ligand framework to couple the targeting molecule. These extremely rigid N-donor ligands efficiently encapsulate Cu(II) leading to octahedral complexes that present stability constants in the same range as those of macrocyclic Cu(II) complexes. Also, these acyclic ligands still keep relatively fast complexation kinetics like other open-chain amine-pyridine based ligands. These favorable features prompted the synthesis of the model complex ^{64}Cu -bispidine and its *in vitro* evaluation. No transchelation or demetalation was found in the presence of superoxide dismutase (SOD) or in rat plasma.⁶⁶

Square planar bis(thiosemicarbazone) Cu(II) complexes were explored for the development of ^{64}Cu radiopharmaceuticals several years ago (Fig. 4). Specifically, ^{64}Cu -ATSM (ATSM: diacetyl-bis(N^4 -methylthiosemicarbazone)) has been considered a promising hypoxia-specific PET tracer.⁶⁷

Recently, a new ATSM derivative bearing a pendant hexanoic acid arm (ATSM-Ahx) was synthesized (Fig. 4), conjugated to a bombesin analog and labeled with ^{64}Cu .⁶⁸ *In vitro* studies have shown that the resulting radiometallated peptide resisted to histidine and cysteine challenge. It is of crucial importance to evaluate the *in vivo* stability of such Cu complexes.

Technetium and rhenium

$^{99\text{m}}\text{Tc}$ is among the most widely used SPECT radionuclides for labeling bioactive peptides, due to its ideal nuclear properties, low-cost and availability from commercial $^{99}\text{Mo}/^{99\text{m}}\text{Tc}$ generators. The radiometallation of peptides with $^{99\text{m}}\text{Tc}$ is done in aqueous solution, starting from the Tc(VII) permethylate anion ($^{99\text{m}}\text{TcO}_4^-$), which needs to be reduced prior to its complexation by an adequate BFC carrying the biomolecule. The diverse and rich chemistry of this radiometal allows the use of different strategies for labeling

peptides with $^{99\text{m}}\text{Tc}$, in terms of metal cores and/or oxidation states and selection of BFCs (Fig. 5).^{69–74}

One of the approaches used for labeling peptides with $^{99\text{m}}\text{Tc}$ relies on the use of square-pyramidal Tc(V) oxocomplexes of the type $[\text{TcO}(\text{N}_x\text{S}_{4-x})]$ containing the $[\text{TcO}]^{3+}$ core and tetradentate N_xS_{4-x} bifunctional chelators, namely the tripeptide mercaptoacetiltryglycine (MAG-3) that acts as a N_3S -donor ligand and presents a pendant carboxylic arm for biomolecule coupling (Fig. 5).⁷⁵ This class of complexes can give *syn* and *anti* isomers that may present different biological properties. In addition, the functionalization of the tetradentate chelator with the biologically active molecule can be quite demanding, requiring tedious protection/deprotection strategies. To overcome some of the drawbacks associated with the use of Tc(V) monoxocomplexes, other approaches based on the *trans*- $[\text{TcO}_2]^+$ and the $[\text{Tc-HYNIC}]$ (HYNIC = 6-hydrazinonicotinic acid) cores (Fig. 5) have been exploited, and these approaches led, in several instances, to radiometallated peptides with promising biological profiles. The *trans*- $[\text{TcO}_2]^+$ core has been used in combination with acyclic tetraamine ligands, which form well-defined octahedral Tc(V) dioxocomplexes, and can be C-functionalized with pendant arms suitable for the coupling of peptides, as shown in Fig. 5.⁷⁶ The $[\text{Tc-HYNIC}]$ core offers the advantage of a straightforward functionalization with the biomolecule, avoiding the use of tedious and time-consuming protection strategies. HYNIC can coordinate as a uni- or bidentate ligand and, therefore, does not fulfill the coordination requirements of the metal, making necessary the use of chelating coligands. Hydrophilic N- and O-donors, like ethylenediamine diacetic acid (EDDA), gluconate or tricine, are among the most explored coligands.^{74,77–79} The use of such coligands offers the advantage of an easy adjustment of the physico-chemical properties (*e.g.* charge, hydrophilicity) of the final complexes, which can strongly influence the pharmacokinetics and excretory pathways of $^{99\text{m}}\text{Tc}$ -labeled peptides. However, the resulting binary mixed-ligand complexes show a relatively low stability. The improvement of the stability of Tc-HYNIC complexes has been achieved by the introduction of a ternary ligand, such as a water-soluble phosphine, or by exploring phosphine- and nicotinyl-containing HYNIC chelators.^{79–82} The nature of the Tc–N bonds involved in the coordination of HYNIC is still unknown, which can be a serious drawback since the full characterization and chemical identification of a potential radiopharmaceutical is mandatory to get a marketing authorization. The so-called tricarbonyl approach has gained considerable attention in the last few years, following the introduction by Alberto and co-workers of a convenient and fully aqueous-based kit preparation of the organometallic precursor *fac*- $[\text{Tc}(\text{CO})_3(\text{OH})_3]^+$ directly from $[\text{TcO}_4]^-$.^{83,84} The chemical robustness of the *fac*- $[\text{Tc}(\text{CO})_3]^+$ core and the lability of the three water molecules offer the possibility of exploring a

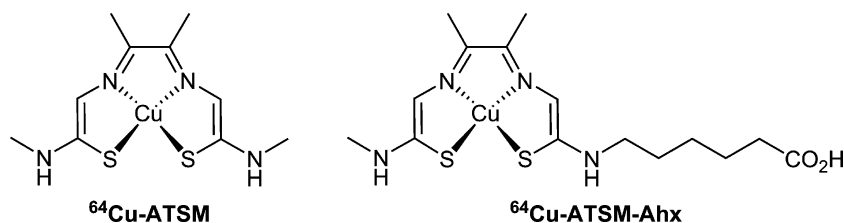


Fig. 4 Bis(thiosemicarbazone) Cu(II) complexes.

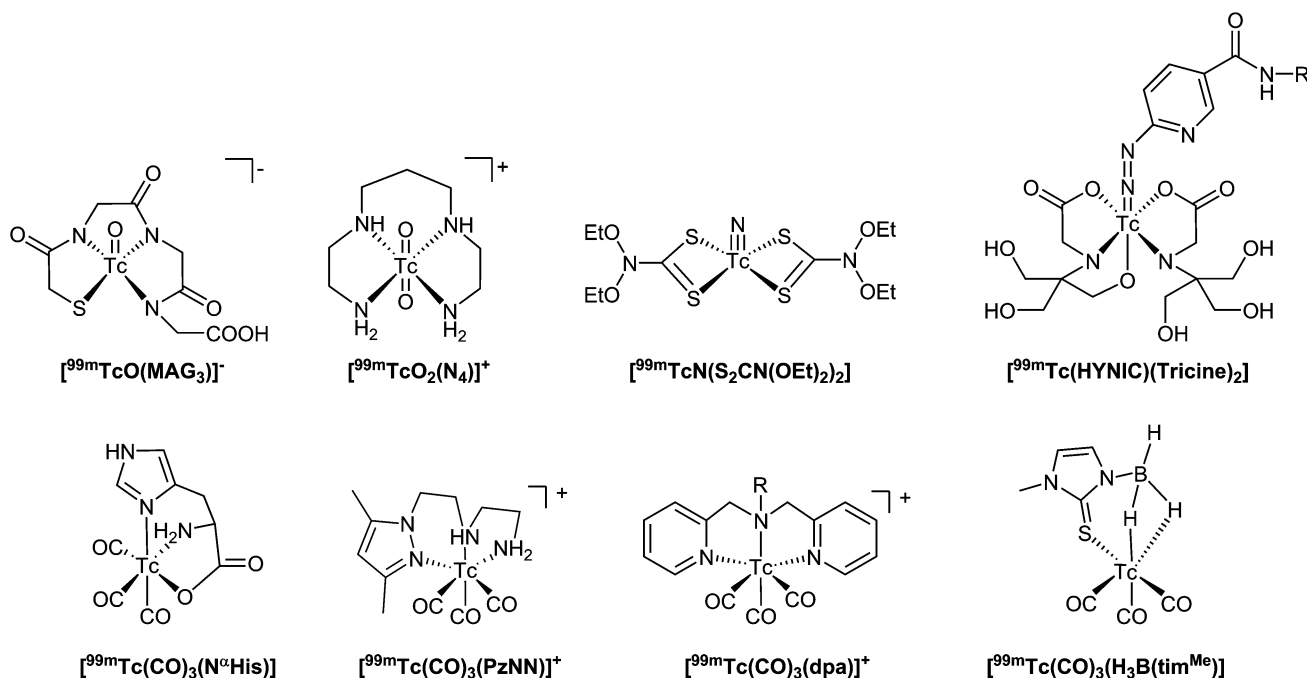


Fig. 5 Selected ^{99m}Tc -complexes with different cores, oxidation states and BFCs.

well-defined chemistry that is easily amenable to bioconjugation. Labeling of peptides based on this organometallic approach has been reported by several research groups, using bidentate or tridentate BFCs.^{69–74} In general, complexes anchored by tridentate chelators are more stable *in vivo* compared with those involving bidentate BFCs (Fig. 5).

Rhenium has two β -emitting isotopes, ^{186}Re and ^{188}Re (Table 1), with nuclear properties suitable for the development of therapeutic radiopharmaceuticals, namely for TRT. The chemistry of rhenium is quite similar to that of the 7th group congener technetium, in terms of the large variety of oxidation states, metallic cores, and bifunctional chelators adequate for the design of radiopharmaceuticals.^{71,85} In fact, for a given class of ligands and metal oxidation state, Re and Tc complexes are usually isostructural. However, there are important differences in the kinetics of ligand exchange reactions and redox chemistry of Re and Tc complexes, which are key issues in the radiopharmaceutical chemistry of these metals. Rhenium compounds are more difficult to reduce than the Tc congeners. Moreover, ligand exchange reactions are faster for Tc complexes. The labeling of peptides with $^{186}\text{Re}/^{188}\text{Re}$ can be attempted using the strategies mentioned above for ^{99m}Tc , starting from aqueous perrhenate. However, the achievement of ^{186}Re and ^{188}Re -labeled peptides with high *in vivo* stability can be quite challenging due to more pronounced tendency of Re complexes to undergo *in vivo* oxidation reactions.

Target-specific radiometallated peptides

Radiopeptides targeting the $\alpha_v\beta_3$ integrin receptor

Integrins are a family of heterodimeric receptors that play a pivotal role in many cell–cell and cell–extracellular matrix interactions.^{86,87} They consist on transmembrane glycoproteins that contain two non-covalently bound α and β subunits. In mammals, 18 α and

8 β subunits have been characterized, which selectively combine to afford at least 24 different integrin receptors.⁸⁸ The integrin receptor $\alpha_v\beta_3$, also known as the vitronectin receptor, is expressed on endothelial cells and modulates cell migration and survival during angiogenesis. Being overexpressed in a variety of tumor cell types, such as glioblastoma, melanoma, ovarian, breast and prostate cancer, it potentiates tumor invasion and metastasis.^{89–92} Thus, the $\alpha_v\beta_3$ receptor has become a target of choice for the diagnosis and therapy of rapidly growing and metastatic tumors.⁹³ Additionally, the non-invasive assessment of $\alpha_v\beta_3$ expression *in vivo* can be helpful to select patients likely to respond to treatment with antiangiogenic drugs, as well as allowing treatment follow-up.

The $\alpha_v\beta_3$ -integrin recognizes selectively extracellular matrix proteins, such as vitronectin or fibronectin, which contain the exposed Arg–Gly–Asp (RGD) sequence.⁹⁴ The discovery of the canonical RGD sequence motivated an intense research work on small peptide-based molecules aimed at finding $\alpha_v\beta_3$ -integrin antagonists suitable for antiangiogenic therapy.^{95,96} Moreover, a plethora of mono- and multivalent RGD-containing peptides have been labeled with a variety of radionuclides.^{97–102} So far, the most promising results have been obtained with [^{18}F]galacto-RGD,¹⁰³ which has been evaluated in patients with melanoma, sarcoma and breast cancer. However, this tracer has a relatively low tumor uptake, high cost and is obtained by a tedious and relatively low-yield radiosynthesis. Looking for a better alternative, intense research efforts have been devoted to radiometallated RGD-containing peptides for PET or SPECT imaging of $\alpha_v\beta_3$ -integrin receptors.

Incorporation of the RGD sequence into a cyclic pentapeptide structure provides $\alpha_v\beta_3$ -antagonists with enhanced affinity and selectivity, as in the case of cyclo(Arg–Gly–Asp–D–Tyr–Val). Replacement of the Val⁵ in c(RGDfV) by Lys led to c(RGDfK) (Fig. 6) without altering the integrin $\alpha_v\beta_3$ binding-affinity.^{104,105}

The c(RGDfK) motif has been the most extensively explored for development of radiometallated peptides, profiting from the presence of the ϵ -NH₂ group of Lys⁵ to conjugate to a BFC and/or pharmacokinetic modifiers (Fig. 6). For evaluation of compounds with maximized binding affinity *via* the bivalency/multivalency approach, the c(RGDfK) motif has also been used to synthesize congener multimeric molecules (*e.g.* E[c(RGDfK)]₂ or E[E[c(RGDfK)]₂]₂) *via* either a glutamic acid tree, by assembling to the Regioselectivity Addressable Functionalized Template (RAFT), or by click chemistry (Fig. 6).^{106–117}

The linear peptides Gly¹-Arg²-Gly³-Asp⁴-Ser⁵-Pro⁶-Cys⁷ and Arg¹-Gly²-Asp³-Ser⁴-Cys⁵-Arg⁶-Gly⁷-Asp⁸-Ser⁹-Tyr¹⁰ were the first ^{99m}Tc-labeled RGD-containing compounds.^{118,119} The resulting radiometallated peptides correspond most likely to Tc(v) oxocomplexes stabilized by the cysteine side chain. The radiolabeled decapeptide was able to localise metastatic melanoma lesions in several patients but with low tumor-to-background ratios.¹¹⁹ A doubly cyclized RGD-containing peptide (NC100692), bearing a PEGylated C-terminus and a diamine-dioxime chelator for complexation of Tc(v), was used to prepare ^{99m}Tc-NC100692 (Fig. 7).^{120–122} The ability of ^{99m}Tc-NC100692 to detect metastatic lesions in 15 patients with lung cancer and 10 patients with breast cancer was investigated in a multicenter

phase 2a clinical trial. It has been concluded that the sensitivity of ^{99m}Tc-NC100692 to detect liver metastases was poor and the detection of bone metastases equivocal. However, lung and brain metastases from both breast and lung cancer could be detected.¹²²

Different monomeric or multimeric cyclic RGD-containing peptides have been labeled with ^{99m}Tc using the HYNIC approach.^{97,99} The ^{99m}Tc complex ^{99m}Tc-HYNIC-E[c(RGDfK)]₂ has shown a tenfold higher affinity for $\alpha_v\beta_3$ -integrin compared to the monomeric congener ^{99m}Tc-HYNIC-E-c(RGDfK). In agreement, the dimeric compound has shown an increased tumor uptake and retention in a OVCAR-3 ovarian carcinoma xenograft. However, kidney retention of the dimeric peptide was higher than that of the corresponding monomer.^{107,123} To improve the biodistribution profile of radiolabeled dimeric peptides of the ^{99m}Tc-HYNIC-E[c(RGDfK)]₂ type, different strategies were explored, namely the use of different co-ligands such as trisodium triphenylphosphine-3,3',3''-trisulfonate (TPPTS), isonicotinic acid (ISONIC) or 2,5-pyridinedicarboxylic acid (PDA). The resulting ternary complexes, [^{99m}Tc-HYNIC-E[c(RGDfK)]₂(tricine)(L)] (L = TPPTS, ISONIC, PDA) showed a high tumor uptake and improved tumor to kidney and tumor to liver ratios.¹²⁴

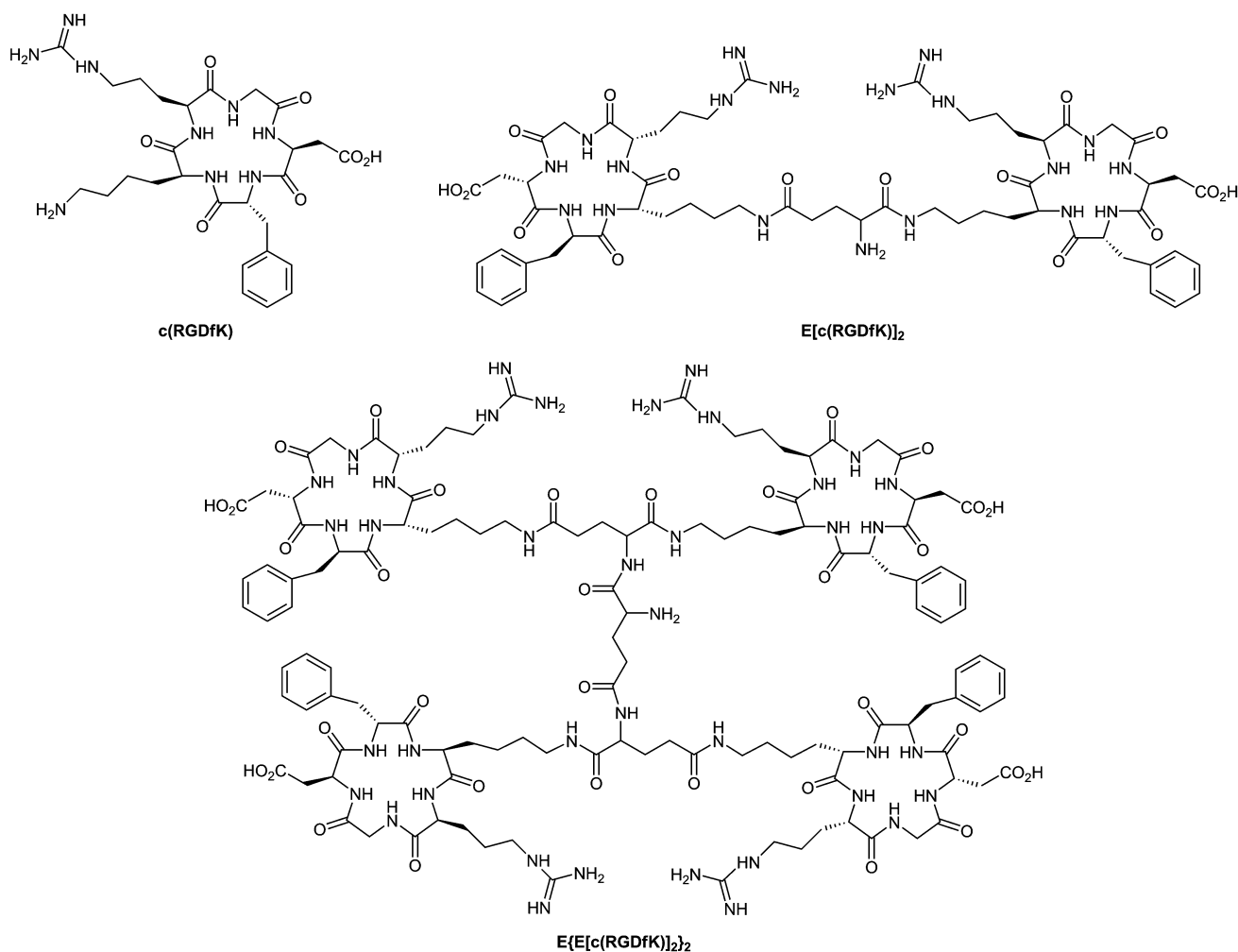


Fig. 6 Monomeric, dimeric and tetrameric cyclic RGD peptides.

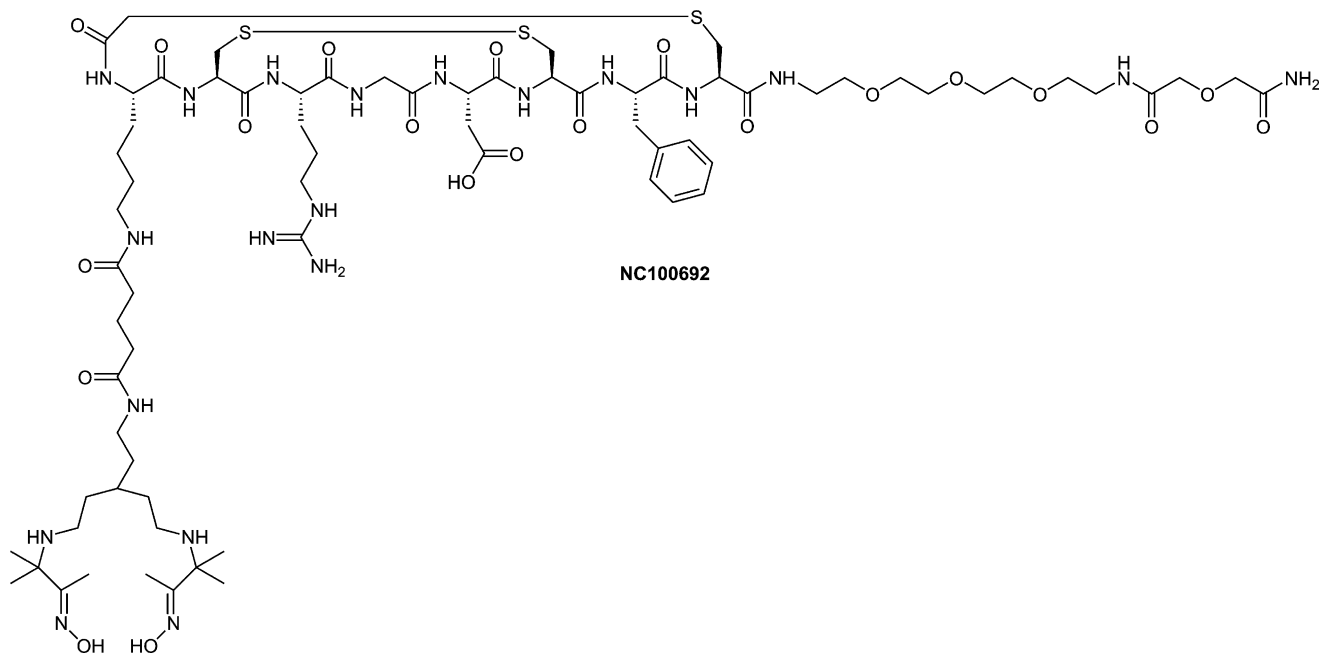


Fig. 7 Structure of NC100692.

A series of cyclic dimeric RGD peptides containing triglycine (G_3) and PEG₄ linkers between the E[c(RGDfK)₂] binding motifs were recently introduced and labeled with ^{99m}Tc using the HYNIC approach and TPPTS as the co-ligand. The complexes [^{99m}Tc(HYNIC-3G₃-dimer)(tricine)(TPPTS)] and [^{99m}Tc(HYNIC-3PEG₄-dimer)(tricine)(TPPTS)] have shown a higher $\alpha_v\beta_3$ -integrin binding affinity and much higher tumor uptake in MDA-MB-435 breast cancer xenograft than [^{99m}Tc(HYNIC-PEG₄-dimer)(tricine)(TPPTS)].^{125,126} These differences can be accounted for by the longest distances between the two cyclic RGD motifs providing for the best-performing complex. The related radiopeptide [^{99m}Tc(HYNIC-PEG₄-tetramer)(tricine)(TPPTS)], bearing a tetrameric RGD derivative, also presented a high tumor uptake, but has shown more pronounced kidney and liver retention compared to the dimeric congeners.

The tricarbonyl approach has been also used in several instances for labeling linear or cyclic RGDf/yK peptides, using histidine, *N,N*-picolyamine diacetic acid (PADA), iminodiacetic acid (IDA) or pyrazolyl-diamine (pzNN) as BFCs.^{127–129} The radiometallation of RGD-containing peptides did not compromise their affinity for $\alpha_v\beta_3$ -integrin receptors, although all the compounds presented a relatively low tumor accumulation.

A variety of monomeric or multimeric RGD-containing peptides have been labeled with ¹¹¹In, ⁶⁸Ga and ⁶⁴Cu, using polyaminocarboxylic ligands as BFCs. The initial studies were done with DTPA- and DOTA-c(RGDf/yK) derivatives, which were further optimized using pharmacokinetic modifiers such as additional charged amino acids (e.g. glutamic acid) or PEGylated linkers.^{130,131} In the case of [¹¹¹In-DTPA-*E*-E[c(RGDfK)₂]] and [⁶⁴Cu-DOTA-PEG(3400)-c(RGDfK)] the presence of glutamic acid and PEG (3400 Da) spacers led to enhanced tumor to kidney, and tumor to liver ratios without compromising tumor uptake.^{113,132} Some dimeric RGD derivatives (Fig.6) were coupled to NOTA and DOTA chelators, using triglycine (G₃) or PEG₄

linkers, and labeled with ⁶⁸Ga, ⁶⁴Cu or ¹¹¹In. The radioconjugates [⁶⁸Ga-NOTA-X-dimer] (X = 2G₃, 2PEG₄), [M-DOTA-3PEG₄-dimer] and [M-DOTA-3G₃-dimer] (M = ⁶⁴Cu, ¹¹¹In) have shown high tumor uptake and prolonged tumor retention with favorable tumor to background ratios.^{133–136} Interestingly, [⁶⁴Cu-DOTA-3PEG₄-dimer] and [¹¹¹In-DOTA-3PEG₄-dimer], sharing the same BFC, have shown almost superimposed tumor uptake and tumor to background values in the same animal model, suggesting a minimal impact of the radiometal on the biodistribution profile.^{133,135} [¹¹¹In-DTPA-3PEG₄-dimer] has also shown a high initial tumor uptake with excellent tumor-to-liver and tumor-to-kidney ratios. However, the DTPA-conjugate showed a much faster tumor washout and poorer tumor-to-background ratios compared to [¹¹¹In-DOTA-3PEG₄-dimer].¹³⁵ Altogether, these findings seem to indicate that 3PEG₄-dimer and 3G₃-dimer are among the most suitable RGD-containing compounds to design radiometallated peptides for SPECT and PET imaging of $\alpha_v\beta_3$ -integrin expression, as well as for PRRT (Peptide Receptor Radionuclide Therapy) of $\alpha_v\beta_3$ -positive tumors.

Radiopeptides targeting the cholecystinin 2 (CCK2)/gastrin receptor

Cholecystinin (CCK) is an endogenous regulatory peptide that displays a wide variety of physiological functions both in the gastrointestinal tract and central nervous system. All the biologically active forms of the peptide (e.g. CCK33, CCK8 and CCK4) are derived from a 115-amino acid peptide precursor, with CCK8 (Asp-Tyr-Met-Gly-Trp-Met-Asp-Phe-NH₂) being the most abundant form in the brain.^{137–139} So far, three distinct subtypes of CCK receptors have been identified: CCK1 or CCK-A, CCK2/gastrin receptor or CCK-B, and CCK2idsv.^{137–140} A high incidence of CCK2 receptor protein was found in medullary thyroid carcinomas (MTC) (92%), small cell lung cancer (SCLC)

(89%), stromal ovarian cancers (100%), astrocytomas (65%), some of the neuroendocrine gastroenteropancreatic tumors, and in several soft tissue tumors, in particular in leiomyosarcomas.^{2,141,142}

Thorough research efforts have been directed toward the development of radioactive peptides for targeting CCK2 receptor *in vivo*, aiming at the visualization/detection or treatment of CCK2 receptor-expressing tumors such as MTC or SCLC.^{143–145}

As can be seen in Tables 3 and 4, the peptides studied include gastrin- or CCK-related analogs, which share the C-terminal CCK receptor-binding tetrapeptide sequence Trp-Met-Asp-Phe-NH₂. In some of these analogs, the methionine amino acid may be replaced by leucine or norleucine.¹⁴⁵

The initial promising results obtained with ¹³¹I-labeled gastrin I at the preclinical and preliminary clinical level prompted several

research groups to label gastrin and CCK analogs with metals such as ¹¹¹In or ^{99m}Tc using adequate BFCs.^{146,147}

Behr and Béhé demonstrated that [¹¹¹In-DTPA-DGlu¹]MG ([¹¹¹In-DTPA-MG0) showed improved *in vitro* and *in vivo* stability over [¹¹¹In-DTPA-JMG].¹⁴⁷ In tumor-bearing nude mice, fast and specific uptake in CCK-B-receptor-positive tissues and a fast renal clearance pattern was found for both peptides. However, [¹¹¹In-DTPA-JMG showed higher background activity in the whole body. In humans, fast tumor and stomach uptake was observed for both ¹¹¹In-labeled compounds, but ¹¹¹In-DTPA-MG0 lacked the liver, spleen and bone marrow uptake observed with its Leu¹ analog.¹⁴⁸

Following a preliminary pilot clinical study with ¹¹¹In-DTPA-MG0 in four MTC patients, where CCK2 receptor expression was identified both in physiologically CCK2 receptor-expressing tissues and in metastatic lesions, a larger clinical study in 75 patients was performed.^{147,149} These clinical studies allowed the visualization of all tumors detected by other imaging modalities and, interestingly, in 29 out of 32 MTC patients with occult disease, at least one lesion was detected. In the same study, the therapeutic effect of ⁹⁰Y-DTPA-MG0 was studied in 8 MTC patients and, despite severe nephrotoxicity in two of them, four patients experienced stabilization of the disease, which lasted for up to 36 months. The utility of ¹¹¹In-DTPA-MG0 for visualization of CCK2 receptor-expressing tumors was confirmed by an independent clinical study conducted by Gottardt *et al.*¹⁵⁰

Aiming to reduce the high renal retention associated with MG0, the MG11, minigastrin analogs, missing five glutamic acid residues in positions 2–6, have been developed. The biological properties of ¹¹¹In-DTPA-MG0 were also compared with those of the radiopetide ¹¹¹In-DOTA-MG11 in AR4-2J-tumor bearing Lewis rats. The reduction of the number of glutamates increased tumor-to-kidney ratio but, additionally, resulted also in a considerably lower metabolic stability.^{151,152}

A new family of ¹¹¹In- DOTA-minigastrin analogs, containing a variable number of His residues at the N-terminal (¹¹¹In-DOTA-H2Met, ¹¹¹In-DOTA-H2Nle, ¹¹¹In-DOTA-H6Nle) was assessed in pancreatic xenografted models (Table 3).¹⁵³ Among these peptides, ¹¹¹In-DOTA-H2Met has shown the most interesting properties in terms of tumor-to-kidney ratios, with saturable uptake in target organs and low uptake by nontarget tissues other than the kidney. However, a high level of oxidation of the methionine residues was observed during the labeling procedure. Replacement of Met by Nle, a non-oxidizable amino acid, led to a significant reduction of receptor affinity and *in vivo* tumor uptake, contrary to what has been described for other analogs.^{154,155}

To improve the *in vivo* performance of these monomeric CCK2R-binding minigastrin analogs, Sosabowski *et al.* labeled the divalent gastrin peptide conjugate DOTA-Gly-Ser-Cys(succinimidopropionyl-Glu-Ala-Tyr-Gly-Trp-Nle-Asp-Phe-NH₂)-Glu-Ala-Tyr-Gly-Trp-Nle-Asp-Phe-NH₂ (DOTA-MGD5) with ¹¹¹In, and compared the tumor-targeting properties of the resulting radiocomplex with those of ¹¹¹In-DOTA-H2Met. Biological studies have shown that dimerization of the receptor binding site resulted in an increase in tumor uptake. However, such effect must still be confirmed in humans.^{156,157}

One of the most successful approaches to target CCK2 receptor-expressing tumors *in vivo* with radiometal-based probes has been developed by Nock *et al.*, who synthesized a minigastrin analog labeled with the *trans*-[^{99m}TcO₂]⁺ core stabilized by a tetraamine

Table 3 Gastrin and gastrin analogs^a

Amino acid sequence:

pGlu-Gly-Pro-Trp-Leu-(Glu)₅-Ala-Tyr-Gly-Trp-Met-Asp-Phe-NH₂ (**Human Gastrin I**)
 Leu-(Glu)₅-Ala-Tyr-Gly-Trp-Met-Asp-Phe-NH₂ (**Minigastrin (MG)**)
 DGlu-(Glu)₅-Ala-Tyr-Gly-Trp-Met-Asp-Phe-NH₂ (MG0)
 DGlu-Ala-Tyr-Gly-Trp-Met-Asp-Phe-NH₂ (MG11)
 His-His-Glu-Ala-Tyr-Gly-Trp-Met-Asp-Phe-NH₂ (H2Met)
 His-His-Glu-Ala-Tyr-Gly-Trp-Nle-Asp-Phe-NH₂ (H2Nle)
 (His)₆-Glu-Ala-Tyr-Gly-Trp-Nle-Asp-Phe-NH₂ (H6Nle)
 Gly-Ser-Cys(succinimidopropionyl-Glu-Ala-Tyr-Gly-Trp-Nle-Asp-Phe-NH₂)-Glu-Ala-Tyr-Gly-Trp-Nle-Asp-Phe-NH₂ (divalent peptide MGD5)
 Gly-DGlu-(Glu)₅-Ala-Tyr-Gly-Trp-Met-Asp-Phe-NH₂ ([Gly⁰-DGlu¹]MG)



Glu-Ala-Tyr-Gly-Trp-Met-Asp-Phe-NH₂ (**Peptide1**)
 Gly-His-Glu-Ala-Tyr-Gly-Trp-Met-Asp-Phe-NH₂ (**Peptide2**)
 Gly-Ala-Tyr-Gly-Trp-Met-Asp-Phe-NH₂ (**Peptide3**)

^a Amino acid residues in bold type are important for the biological activity of the peptide.

Table 4 Cholecystokinin (CCK) analogs^{a,b}

Amino acid sequence:

DAsp-Tyr-Met-Gly-Trp-Met-Asp-Phe-NH₂ (**CCK8**)
 DAsp-Tyr(OSO₃H)-Met-Gly-Trp-Met-Asp-Phe-NH₂ (**sCCK8**)
 DAsp-Tyr-Nle-Gly-Trp-Nle-Asp-Phe-NH₂ ([Nle^{3,6}]CCK8; **CCK8(Nle)**)
 DAsp-Phe(*p*-CH₂SO₃H)-Nle-Gly-Trp-Nle-Asp-Phe-NH₂ (**sCCK8[Phe²(*p*-CH₂SO₃H), Nle^{3,6}]**)
 DAsp-Phe(*p*-CH₂SO₃H)-HPG-Gly-Trp-HPG-Asp-Phe-NH₂ (**sCCK8[Phe²(*p*-CH₂SO₃H), HPG^{3,6}]**)
 Trp-Nle-Asp-Phe-NH₂ (**CCK4**)
 Ahx-Ahx-Trp-Nle-Asp-Phe-NH₂ ((Ahx)₂-**CCK4**)
 DAsp-Tyr-Met-Gly-Trp-Nle-Asp-Phe-NH₂ ([Nle⁶]CCK8)

^a HPG = homopropargylglycine; Ahx = 6-aminoheptanoic acid. ^b Amino acid residues in bold type are important for the biological activity of the peptide.

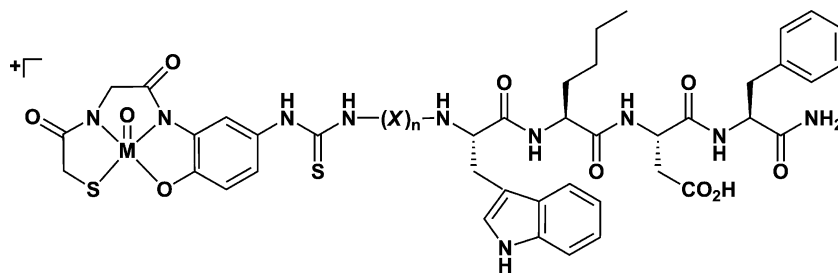


Fig. 8 Metallated CCK4 derivatives of the type $[M(O)(SN_2O-PhSCN-X_n-CCK4)]$ ($M = {}^{99m}Tc, Re$; $X = \beta$ -alanine, Ahx; $n = 0, 2$ and 4).

ligand. Different spacers between the chelator and the peptide have been explored. Among all of them, $[{}^{99m}Tc(O_2)(N_4^{0-1})Gly^0-DGlu^1]MG$ (Demogastrin 2) was the most promising. The biological behavior of Demogastrin 2 has been compared with that of ${}^{111}In$ -DOTA-MG11 and ${}^{111}In$ -DOTA-CCK8 both at the preclinical and clinical level. Demogastrin 2 was the best diagnostic tool in MTC patients, not only because of its superior *in vivo* stability, but also due its high sensitivity and better quality of the scintigraphic images. Renal uptake was similar to all radiopeptides studied, but could be reduced by co-injection of polyglutamic acid.¹⁵⁸⁻¹⁶⁰

The analogs MG0 and MG11 were also labeled with ${}^{99m}Tc$, using the HYNIC approach, and the resulting complexes, ${}^{99m}Tc$ -EDDA-HYNIC-MG0 and ${}^{99m}Tc$ -EDDA-HYNIC-MG11, were evaluated in AR4-2J rat pancreatic tumor cells and in AR4-2J tumor-bearing nude mice. The ${}^{99m}Tc$ -EDDA-HYNIC-MG11 derivative showed advantages over ${}^{99m}Tc$ -EDDA-HYNIC-MG0, in terms of lower kidney retention with unchanged uptake in tumors and CCK-2 receptor-positive tissue. However, the lower metabolic stability and impurities formed in the labeling process still leave room for further improvement.¹⁶¹ Attempting to improve stability, cyclic variants of MG11 have been proposed, and the resulting peptides were labeled with the ${}^{99m}Tc$ -HYNIC moiety, yielding the radiometalated peptides ${}^{99m}Tc$ -EDDA-HYNIC-cycloMG1 and ${}^{99m}Tc$ -EDDA-HYNIC-cycloMG2. Both radiopeptides showed rapid internalization in receptor expressing cells (AR42J cells) and high tumor uptake in AR42J tumor xenografts. However, the cyclization of MG had only a limited effect on the overall stability, and the biodistribution profile of ${}^{99m}Tc$ -EDDA-HYNIC-cyclo-MG1 was similar to the linear analog ${}^{99m}Tc$ -EDDA-HYNIC-MG11.¹⁶²

King *et al.* reported the synthesis of three peptide-HYNIC conjugates containing the -Ala-Tyr-Gly-Trp-Met-Asp-Phe-NH₂ C-terminal sequence and combinations of histidine, glutamic acid, and glycine. The peptide conjugates were labeled with ${}^{99m}Tc$ using either tricine or EDDA as a coligand, and their biological properties evaluated in AR42J cells and AR42J tumor xenograft. It was found that the insertion of histidine into the sequence of peptide-HYNIC conjugates resulted in more stable, more homogeneous ${}^{99m}Tc$ complexes (${}^{99m}Tc$ -Tricine-HYNIC-Lys-Peptide2) (Table 3), with improved tumor-targeting performance both *in vitro* and *in vivo*.¹⁶³

In addition to the previously mentioned radioiodination studies of gastrin analogs for targeting CCK receptors *in vivo*, Beher *et al.* also investigated the utility of CCK derivatives, and concluded that sulfated (s) CCK analogs and some non-sulfated (ns) gastrin analogs displayed the highest binding affinities (Tables 3 and 4). Desulfation or the complete removal of the N-terminal Tyr led to a loss of affinity.¹⁴⁷

Reubi *et al.* has introduced a family of highly potent and selective DTPA- and DOTA-CCK (non-sulfated) analog conjugates: DTPA-CCK8(Nle) and DTPA-CCK8. The corresponding ${}^{111}In$ complexes were prepared, and their biological properties indicated that these compounds have substantial promise for the *in vivo* visualization of CCK-B receptor-expressing tumors.¹⁵⁴ Only ${}^{111}In$ -DOTA-CCK8(Nle) was evaluated in humans and it was shown that this complex holds great potential for both scintigraphy and radionuclide therapy of human CCK2 receptor positive tumors such as MTC and SCLC.¹⁶⁴

More recently, Aloj *et al.* studied the *in vitro* and *in vivo* properties of ${}^{111}In$ -DTPAGlu-Gly-CCK8, a complex containing the chelating moiety DTPAGlu bound through a glycine linker at the N-terminal end of the bioactive peptide CCK8. It was found that this highly stable radiopeptide presents a high-binding affinity to the receptor and presented avid uptake in CCK2R overexpressed xenografts, with rapid clearance of unbound radioactivity through the kidneys.^{146,165}

The radiopeptide ${}^{111}In$ -BPCA-(Ahx)₂-CCK4, which contains two 6-aminohexanoic acid (Ahx) moieties between the BFC (BPCA) and the CCK4 derivative, presented a high and specific tumor uptake and a low renal accumulation in mice bearing E151A-CCK2R tumors compared with the internal control, ${}^{111}In$ -*trans*-cyclohexyldiethylenetriaminepentaacetic acid cholecystokinin octapeptide (${}^{111}In$ -SCN-CHX-A''-DTPA-[Nle]⁶-CCK8).¹⁶⁶ The same research team has also proposed a set of ${}^{99m}Tc$ (v)-radiolabelled short peptide conjugates of the type indicated in Fig. 8.¹⁶⁷

Laverman *et al.* have shown that sulfated and non-sulfated CCK8 peptides labeled with the ${}^{99m}Tc$ -HYNIC moiety using tricine/nicotinic acid as coligands bind with high affinity to the CCK2 receptor. ${}^{99m}Tc$ -HYNIC-sCCK8 also showed high affinity toward the CCK1 receptor. Studies in athymic mice bearing subcutaneous tumors expressing either CCK1 or CCK2 receptors revealed that uptake of ${}^{99m}Tc$ -HYNIC-sCCK8 in CCK1 or CCK2 receptor-positive tumors was fifteen-fold higher than that of ${}^{99m}Tc$ -HYNIC-nsCCK8.¹⁶⁸

Owing to the fact that sCCK8 contains an easily hydrolyzable sulfated tyrosine residue and two methionine residues prone to oxidation, Roosenburg *et al.* replaced the Tyr(OSO₃H) moiety in sCCK8 by a robust isosteric sulfonate, Phe(*p*-CH₂SO₃H), and replaced the methionine by norleucine (Nle) or homopropargylglycine (HPG). The peptides sCCK8[Phe²(*p*-CH₂SO₃H),Met^{3,6}], sCCK8[Phe²(*p*-CH₂SO₃H),Nle^{3,6}], and sCCK8[Phe²(*p*-CH₂SO₃H),HPG^{3,6}] were N-terminally conjugated to DOTA and labeled with ${}^{111}In$. Biodistribution studies in mice with AR42J tumors showed

[¹¹¹In-DOTA-sCCK8[Ph^e(*p*-CH₂SO₃H),Nle^{3,6}]] to have the highest tumor uptake.¹⁵⁵

CCK8 has been derivatized with a Cys-Gly unit and labeled with the metal fragment ^{99m}[Tc(N)(PNP₃)₂]⁺ (PNP₃ = *N,N*-bis(dimethoxypropylphosphinoethyl)methoxyethylamine), giving the complex [^{99m}Tc(N)(NS-Cys-Gly-CCK8)(PNP₃)₂]⁺. Biodistribution studies in nude mice bearing CCK2-R positive A431 xenografts showed rapid and specific targeting to CCK2-R, a four-fold higher accumulation compared to nonreceptor-expressing tumors.¹⁶⁹

The CCK8 peptide was modified at its N-terminus by addition of two Lys-His units and histidine was coupled to the side chain of the lysine ((Lys-His)₂-CCK8). The conjugate was labeled with *fac*-[^{99m}Tc(CO)₃] and biodistribution experiments showed negligible tumor accumulation in A431-CCK2R xenografts.¹⁷⁰

Radiopeptides targeting the vasoactive intestinal peptide receptor (VPAC-1)

VIP, an endogenous growth hormone, is a 28 amino acid peptide with a wide range of biological activities such as vasodilatation, secretion of different hormones, immunomodulation and proliferation of normal and malignant cells. These actions are mediated through the cell surface receptors VPAC1 and VPAC2, which are expressed in various tissues in different densities.¹⁷¹⁻¹⁷⁴

These receptors, predominantly the VPAC1 subtype, are over-expressed in the great majority of the most frequently occurring human tumors, including breast (100%), prostate (100%), pancreas (65%), lung (58%), colon (96%), stomach (54%), liver (49%), and urinary bladder (100%) carcinomas as well as lymphomas (58%) and meningiomas (100%).¹⁷⁵

VIP or VIP derivatives labeled mainly with ^{99m}Tc, or more recently ⁶⁴Cu, have been explored extensively toward the *in vivo* detection/visualization of VPACR-expressing tumors (Table 5). Aiming to label the VIP peptide with ^{99m}Tc and to assess its properties for imaging colorectal cancer, the peptide was modified at the C-terminal by conjugation to a 4-aminobutyric acid (Aba) spacer, followed by 4 terminal amino acids (Gly-Gly-DAla-Gly),

which provide a N₄ donor atom set for metal stabilization. The pharmacokinetic profile of the resulting labeled peptide (^{99m}Tc-TP3654) (Table 5) was more favorable than that of ¹¹¹In-DTPA-Octreotide or ^{99m}Tc-anti-CEA in the same tumor model. Preliminary clinical studies revealed that within 20 min all of the tumors could be delineated.¹⁷⁶⁻¹⁷⁸

Aimed at targeting VIP/PACAP receptors in breast tumors, a new VIP analog (TP3982) derivatized at the C-terminal with a N₂S₂ chelating unit (-(Dap-(BMA)₂)) has been synthesized and fully characterized. Smooth-muscle relaxivity assays demonstrated functional integrity of the peptide conjugate TP3982, when compared with VIP. The conjugate was labeled with ⁶⁴Cu and ^{99m}Tc in high yields, giving the stable metal-complexes ⁶⁴Cu-TP3982 and ^{99m}Tc-TP3982, respectively. Imaging and tissue distribution studies after injection of ⁶⁴Cu-TP3982, ^{99m}Tc-TP3982 or ^{99m}Tc-TP3654 in nude mice bearing human T47D breast tumor xenografts, revealed a significantly greater (21.2–74-fold) receptor-specific tumor uptake for ⁶⁴Cu-TP3982.¹⁷⁹

Following these promising results, the same team has synthesized and characterized three new VIP analogs (P3939, TP4200 and TP3805) containing also a N₂S₂ chelating unit for metal coordination. The peptide conjugates TP3939, TP4200, TP3805 and TP3982 retained the biological activity as demonstrated by smooth muscle relaxivity assays and cell binding assays (T47T human breast cancer line). The labeling yields of all analogs with ⁶⁴Cu were higher than 92%. *In vitro* receptor autoradiography studies showed 2.17 to 10.93 times greater quantity of ⁶⁴Cu-peptide analogs (including also TP3982) bound to breast cancer tissue (13 human breast cancer tissue) than to the normal breast tissue. These data indicated that a greater number of VPAC1 receptors were expressed on malignant cells than on the normal. This finding was corroborated by RT-PCR studies using the same samples.¹⁸⁰

⁶⁴Cu-TP3939 has been investigated as a PET imaging probe to detect prostate cancer, its metastatic or recurrent lesions and to determine the effectiveness of its treatment. Biodistribution studies in PC3 tumor-bearing nude mice demonstrated rapid blood clearance, high stability and receptor-specific tumor uptake. The PET images delineated the xenografted PC in nude mice, as well

Table 5 Vasoactive intestinal peptide (VIP) and analogs^{a,b}

Amino acid sequence:

His-Ser-Asp-Ala-Val-Phe-Thr-Asp-Asn-Tyr-Thr-Arg-Leu-Arg-Lys-Gln-Met-Ala-Val-Lys-Lys-Tyr-Leu-Asn-Ser-Ile-Leu-Asn-NH ₂ (VIP)
His-Ser-Asp-Ala-Val-Phe-Thr-Asp-Mn-Tyr-Thr-Arg-Leu-Arg-Lys-Gln-Met-Ala-Val-Lys-Lys-Tyr-Leu-Asn-Ser-Ile-Leu-Asn-Aba-Gly-Gly-DAla-Gly (TP3654)
His-Ser-Asp-Ala-Val-Phe-Thr-Asp-Asn-Tyr-Thr-Arg-Leu-Arg-Lys-Gln-Met-Ala-Val-Lys-Lys-Tyr-Leu-Asn-Ser-Ile-Leu-Asn-Aba-Lys-(Dap -(BMA) ₂) (TP3982)
His-Ser-Asp-Ala-Val-Phe-Thr-Asp-Asn-Tyr-Thr-Lys-Leu-Arg-Lys-Gln-Nle-Ala-Val-Lys-Lys-(3-OCH ₃ ,4-OH)Phe-Leu-Asn-Ser-Val-Leu-Thr-Aba-Lys-(Dap -(BMA) ₂) (TP3939)
Ac-His-Ala-Asp-Ala-Val-Phe-Thr-Glu-Asn-Tyr-Thr-Lys-Leu-Arg-Lys-Gln-Nle-Ala-Ala-Lys-c(-Lys-Tyr-Leu-Asn-Asp)-Leu-Lys-Lys-Ala-Ala-Ala-Aba-Lys(Dap -(BMA) ₂) (TP4200)
His-Ser-Asp-Gly-Ile-Phe-Thr-Asp-Ser-Tyr-Ser-Arg-Tyr-Arg-Lys-Gln-Met-Ala-Val-Lys-Lys-Tyr-Leu-Ala-Ala-Val-Leu-Aba-Lys-(Dap -(BMA) ₂) (TP3805)
His-Ser-Asp-Deg-Val-4-Cl-DPhe-Thr-Asp-Asn-Tyr-Thr-Arg-Leu-Arg-Lys-Gln-Leu-Ala-Val-Lys-Lys-Tyr-Leu-Asn-Ser-Ile-Leu-Asn-NH ₂ (VP05)
His-DPhe-Thr-Asp-Asn-Tyr-Thr-Arg-Leu-Arg-Lys-Gln-Leu-Aib-Val-Lys-Lys-Tyr-Leu-NH ₂ (VD4)
His-ACP-DPhe-Thr-Asp-Asn-Tyr-Thr-Arg-Leu-Arg-Lys-Gln-Leu-Aib-Val-Lys-Lys-Tyr-Leu-NH ₂ (VD5)

^a Aba = 4-aminobutyric acid; Dap = diaminopropionic acid. ^b Amino acid residues in bold type are important for the biological activity of the peptide. Some chelating units are also displayed in bold type.

as spontaneous occult PC in TRAMP II mice, which was not delineated by ^{18}F -FDG in the same animal model. As expected, ^{64}Cu -TP3939 did not detect prostate with hyperplasia in TRAMP I, confirming the specific nature of the probe. Brought together, the results confirm the potential of ^{64}Cu -TP3939 for PET imaging of prostate cancer and its metastatic or recurrent lesions.¹⁸¹

Thakur *et al.* also studied the ability of ^{94}Cu -TP3805 to detect breast cancer (BC) in MMTVneu mice using ^{18}F -FDG as a gold standard. PET imaging studies in mice have shown that ^{94}Cu -TP3805 could identify all malignant lesions that overexpressed VPAC1 receptors. Interestingly, benign tumors that did not express the receptor could only be imaged by ^{18}F -FDG and not by ^{94}Cu -TP3805.¹⁸²

A set of three other VIP analogs (VP05, VD4 and VD5) have been directly labeled with the moiety *fac*- $^{99\text{m}}\text{Tc}(\text{CO})_3]^+$, and the tumor-targeting properties of the resulting radioactive species evaluated in human colon carcinoma cells (PTC cells) and in a animal tumor model. Despite the specific *in vitro cell* uptake of $^{99\text{m}}\text{Tc}(\text{CO})_3$ -labeled VP05 analog, its tumor uptake was modest.¹⁸³

Radiopeptides targeting the glucagon-like peptide-1 receptor (GLP-1)

Glucagon-like peptide-1 is a intestinal hormone that plays an important role in glucose metabolism and homeostasis. GLP-1 stimulates postprandial insulin secretion from pancreatic β -cells in a manner dependent on blood-glucose levels. This receptor was shown to be overexpressed in various neuroendocrine tumors, particularly in human insulinomas, as well as in brain tumors and embryonic tumors but not in carcinomas or lymphomas. Additionally, GLP-1R could not be identified in specific tissue compartments of several organs (*e.g.* pancreas, intestine, and lung). Such findings have made this receptor a promising molecular target for *in vivo* imaging or therapeutic proposals.^{184,185}

The proof-of-principle for *in vivo* GLP-1 receptor targeting was provided in a pioneer study by Gottarhardt *et al.*, who detected insulinomas in NEDH rats and RINm5F cells, using radioiodinated GLP-1(7–36)amide and exendin-3 (^{125}I GLP-1(7–36)amide and ^{125}I exendin-3, Table 6).¹⁸⁶ These promising results prompted further studies with radiometallated (^{111}In , ^{68}Ga and $^{99\text{m}}\text{Tc}$) GLP-1 analogs.

DTPA conjugates of exendin-4 were synthesized and labeled with ^{111}In . Among others, the stable radiometallated compound

$[\text{Lys}^{40}(\text{Ahx-DTPA-}^{111}\text{In})\text{NH}_2]\text{exendin-4}$ accumulates significantly and specifically in the tumor of Rip1Tag2 mice, a transgenic mouse model of pancreatic β -cell carcinogenesis, which exhibits a GLP-1R expression comparable with human insulinoma. The high tumor uptake resulted in excellent tumor visualization by pinhole SPECT/MRI and SPECT/CT.^{187,188} The therapeutic potential of $[\text{Lys}^{40}(\text{Ahx-DTPA-}^{111}\text{In})\text{NH}_2]\text{exendin-4}$ has been evaluated also in the same transgenic mouse model (Rip1Tag2 mice). A single injection of the radiopeptide resulted in a reduction of the tumor volume by up to 94% in a dose-dependent manner without significant acute organ toxicity. The authors claim that these results prove that the Auger-emitting compound is able to produce relevant therapeutic effects.¹⁸⁹ The same radiopeptide successfully detected tumors in patients with insulinomas that were not detected by other imaging modalities.¹⁹⁰

Following the successful use of $[\text{Lys}^{40}(\text{Ahx-DTPA-}^{111}\text{In})\text{NH}_2]\text{exendin-4}$ for the detection of insulinomas in rodents and humans, the radiopeptide $[\text{Lys}^{40}(\text{Ahx-DOTA-}^{111}\text{In})\text{NH}_2]\text{exendin-4}$ has been prepared and tested in six patients.¹⁹¹ GLP-1R scans detected the insulinomas in all six cases. By using a γ -probe intra-operatively, the radiopeptide allowed successful surgical removal of all insulinomas, presenting a high density of GLP-1R as confirmed by autoradiography.

To overcome some of the drawbacks associated with the use of ^{111}In for imaging, the new radiopeptides $[\text{Lys}^{40}(\text{Ahx-DTPA-}^{68}\text{Ga})\text{NH}_2]\text{exendin-4}$ and $[\text{Lys}^{40}(\text{Ahx-HYNIC-}^{99\text{m}}\text{Tc/EDDA})\text{NH}_2]\text{exendin-4}$ were prepared. Biodistribution studies in Rip1Tag2 mice have shown a high tumor uptake for $[\text{Lys}^{40}(\text{Ahx-DTPA-}^{68}\text{Ga})\text{NH}_2]\text{exendin-4}$, comparable to that of $[\text{Lys}^{40}(\text{Ahx-DTPA-}^{111}\text{In})\text{NH}_2]\text{exendin-4}$ and significantly higher than that of $[\text{Lys}^{40}(\text{Ahx-HYNIC-}^{99\text{m}}\text{Tc/EDDA})\text{NH}_2]\text{exendin-4}$. However, the lower tumor uptake obtained with the $^{99\text{m}}\text{Tc}$ complex did not result in reduced image quality as all the radiopeptides showed high tumor-to-background ratios. Such results make $^{99\text{m}}\text{Tc}$ - and ^{68}Ga -labeled exendin-4 suitable candidates for clinical GLP-1R imaging studies.¹⁹²

The biodistribution profile of the new radiopeptide $[\text{Lys}^{40}(\text{DOTA-}^{68}\text{Ga})\text{NH}_2]\text{exendin-3}$ was evaluated in BALB/c nude mice with subcutaneous INS-1 tumors and compared with that of $[\text{Lys}^{40}(\text{DOTA-}^{111}\text{In})\text{NH}_2]\text{exendin-3}$ and $[\text{Lys}^{40}(\text{DTPA-}^{111}\text{In})\text{NH}_2]\text{exendin-3}$ in the same animal model. The chelator used did not affect the biodistribution profile of $[\text{Lys}^{40}]\text{exendin-3}$ as evidenced by the almost identical concentrations of $[\text{Lys}^{40}(\text{DOTA-}^{111}\text{In})\text{NH}_2]\text{exendin-3}$ and $[\text{Lys}^{40}(\text{DTPA-}^{111}\text{In})\text{NH}_2]\text{exendin-3}$ in all tissues examined. The biodistribution of the latter was also identical to the biodistribution of $[\text{Lys}^{40}(\text{DTPA-}^{111}\text{In})\text{NH}_2]\text{exendin-4}$. Tumor uptake of ^{68}Ga -labelled $[\text{Lys}^{40}(\text{DOTA})]\text{exendin-3}$ was lower than tumor uptake of ^{111}In -labelled $[\text{Lys}^{40}(\text{DTPA})]\text{exendin-3}$. Despite this difference in insulinoma uptake, the authors claim that clinical studies should be conducted to elucidate the potential of $[\text{Lys}^{40}(\text{Ga-DOTA})]\text{exendin-3}$ for insulinoma PET imaging in Humans.¹⁹³

Peptides targeting chemokine receptor CXCR4

Chemokines are structurally related small glycoproteins (8–14 kDa) that chemoattract leukocytes by binding to cell surface receptors.¹⁹⁴ CXCR4 is highly expressed in breast and prostate cancer, and plays a crucial role in tumor metastasis.^{5,195,196}

Table 6 Glucagon-like peptide 1 (GLP-1) analogs^a

Amino acid sequence:

His-Ala-Glu-Gly-Thr-Phe-Thr-Ser-Asp-Val-Ser-Ser-Tyr-Leu-Glu-Gly-Gln-Ala-Ala-Lys-Glu-Phe-Ile-Ala-Trp-Leu-Val-Lys-Gly-Arg-NH₂
(GLP-1(7–36)amide)
His-Ser-Asp-Gly-Thr-Phe-Thr-Ser-Asp-Leu-Ser-Lys-Gln-Met-Glu₃-Ala-Val-Arg-Leu-Phe-Ile-Glu-Trp-Leu-Lys-Asn-Gly₂-Pro-Ser₂-Gly-Ala-Pro₃-Ser-(Lys⁴⁰)-NH₂ (Lys⁴⁰-Exendin-3)
His-Gly-Glu-Gly-Thr-Phe-Thr-Ser-Asp-Leu-Ser-Lys-Gln-Met-Glu₃-Ala-Val-Arg-Leu-Phe-Ile-Glu-Trp-Leu-Lys-Asn-Gly₂-Pro-Ser₂-Gly-Ala-Pro₃-Ser-(Lys⁴⁰)-NH₂ (Lys⁴⁰-Exendin-4)

^a Amino acid residues in bold type are important for the biological activity of the peptide.

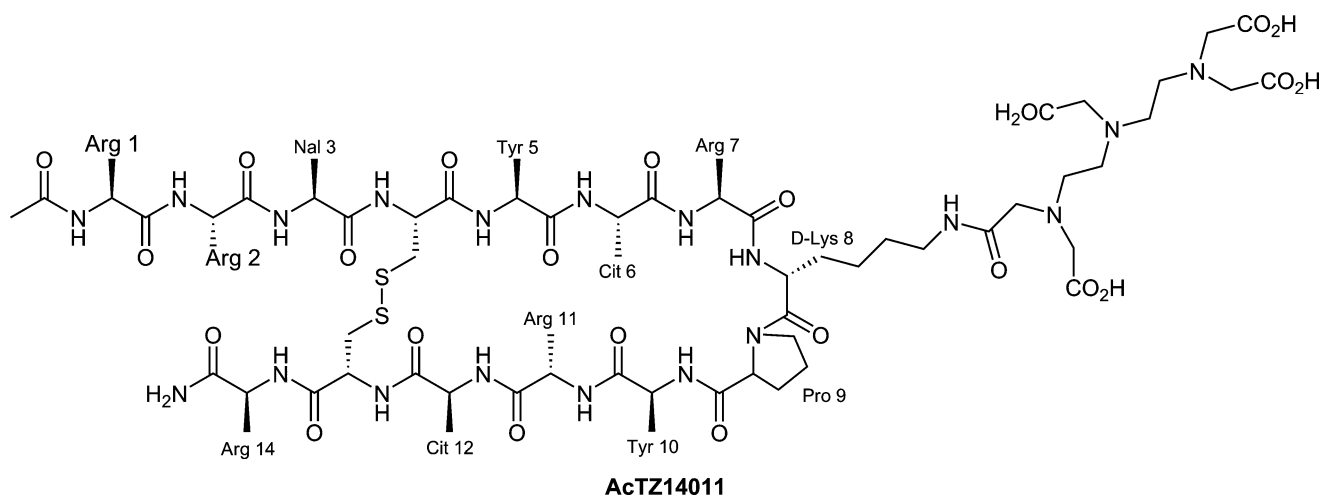


Fig. 9 DTPA–AcTZ14011 peptide conjugate.

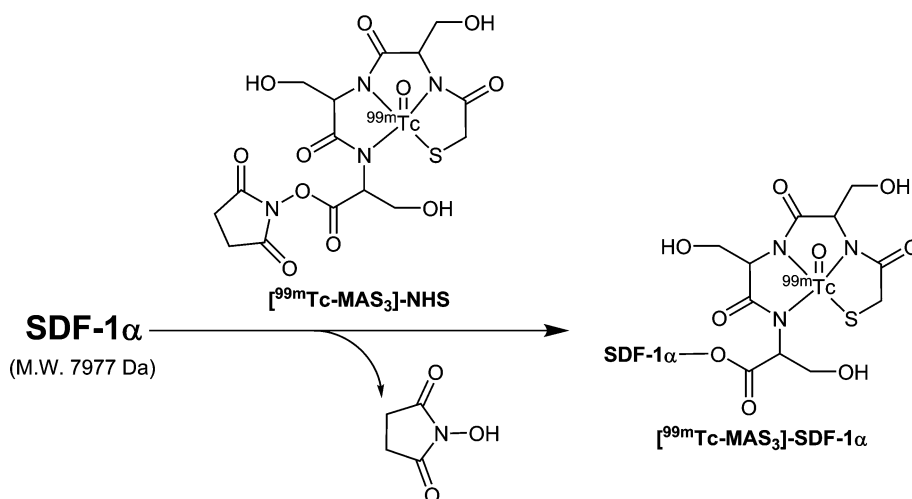


Fig. 10 Labeling of SDF-1 α with ^{99m}Tc.

Additionally, chemokines and their receptors are also associated with cardiac dysfunction.^{197–199}

Aiming to prepare novel radiolabeled probes for the *in vivo* imaging of CXCR4 expression on tumors, Koglin *et al.* radiolabeled CPCR4, a cyclic peptide, and tested its biological properties.²⁰⁰ The authors claim that the tracer binds with high affinity and specificity in an antagonistic manner to its binding site and allowed a clear delineation of CXCR4 positive tumors *in vivo*. However, further optimization of the *in vivo* behavior of the tracer needs to be done.

Hanaoka *et al.* designed a cyclic 14-residue peptidic CXCR4 inhibitor, AcTZ14011 (Fig. 9), attached it to DTPA through the side chain of dLys⁸, and labeled the resulting DTPA–AcTZ14011 conjugate with ¹¹¹In.²⁰¹

Biodistribution studies in nude mice bearing pancreatic carcinoma AsPC-1 have shown that the receptor-specific accumulation of [¹¹¹In-DTPA–AcTZ14011] in the CXCR4-expressing tumor was greater than that in the blood or muscle. The authors claimed that this radiopeptide was a potential radiopharmaceutical for the imaging of CXCR4 expression in metastatic tumors *in vivo*.

Aimed at the non-invasive quantification of CXCR4 expression *in vivo*, for the understanding of its importance in diverse processes including cardiac response to injury, recombinant SDF-1 α was derivatized with a tetradentate N₃S chelator (S-acetylmercaptoacetyltriserine: MAS₃), and labeled with ^{99m}Tc, yielding the highly stable complex [^{99m}Tc-MAS₃]-SDF-1 α (Fig. 10).²⁰²

Biodistribution studies in a rat model of ischemia reperfusion have shown that after induction of myocardial infarction, CXCR4 expression levels in the myocardium increased more than 5-fold, as quantified using [^{99m}Tc-MAS₃]-SDF-1 α and confirmed using confocal immunofluorescence. The main conclusion drawn by the authors is that CXCR4 levels can be quantifiable *in vivo* in a variety of animal models, using appropriate radioactive probes such as [^{99m}Tc-MAS₃]-SDF-1 α .

Peptides targeting neuropeptide Y receptors

Neuropeptide Y (NPY), a member of the pancreatic polypeptide family, consists of 36 amino acids residues and binds to the five Y receptor subtypes (Y1, Y2, Y4, Y5 and y6) with nanomolar

Table 7 Neuropeptide Y (NPY) and analogs^a

Amino acid sequence:

Tyr-Pro-Ser-Lys-Pro-Asp-Asn-Pro-Gly-Glu-Asp-Ala-Pro-Ala-Glu-Asp-Met-Ala-Arg-Tyr-Tyr-Ser-Ala-Leu-Arg-His-Tyr-Ile-Asn-Leu-Ile-Thr-Arg-Gln-Arg-Tyr-NH₂ (**human NPY**)
 Tyr-Pro-Ser-Lys-Pro-Asp-**Phe**-Pro-Gly-Glu-Asp-Ala-Pro-Ala-Glu-Asp-Met-Ala-Arg-Tyr-Tyr-Ser-Ala-Leu-Arg-His-Tyr-Ile-Asn-Leu-Ile-Thr-Arg-**Pro**-Arg-Tyr-NH₂ (**[Phe⁷,Pro³⁴]-NPY**)
 Ile-Asn-**Pro**-Ile-Tyr-Arg-**Leu**-Arg-Tyr-NH₂ (**BVD15**)
 Ile-Asn-**Pro**-Lys-Ile-Tyr-Arg-**Leu**-Arg-Tyr-NH₂ (**[Lys⁴]-BVD15**)
 Ile-Asn-**Pro**-Nle-**Bpa**-Arg-**Leu**-Arg-Tyr-NH₂ (**NPY1**)

^a Amino acid residues in bold type are important for Y1R-binding.

affinity (Table 7).^{203,204} NPY receptors are promising candidates in the oncology field since Y1R and/or Y2R have been found to be expressed in neuroblastoma, breast carcinomas, ovarian cancers, the Ewing sarcoma family of tumors, and high-grade glioblastomas among others.^{205–212} Beck–Sickinger *et al.* labelled a Y2 receptor-preferring NPY analog (Ac-[Ahx⁵⁻²⁴,Lys⁴,Ala²⁶]-NPY) with the organometallic *fac*-[^{99m}Tc(CO)₃]⁺ moiety using PADA (2-picolylamine-*N,N*-diacetic acid) as a chelator. A stable radiopeptide with selective Y2 binding in neuroblastoma cells was obtained.²¹³

With regard to breast cancer, Reubi *et al.* have shown that Y1R is expressed in 85% of all tumors in large quantities and in 100% of the examined metastases.^{211,212} Interestingly, a shift of the receptor subtype from Y2 in healthy tissue to Y1 during neoplasm was found. Thus, Y1R selective peptides have been considered promising for imaging and therapy of breast cancer.^{205,214} A Y1R-specific NPY analog was labelled with ¹¹¹In, using DOTA, and the resulting complex [¹¹¹In-DOTA-Lys⁴,Phe⁷,Pro³⁴]-NPY showed a high kidney and low tumor uptake in MCF-7 breast cancer xenografts.²¹⁵ The same NPY analog was labeled with ^{99m}Tc using a *N*^α-histidinyl acetyl (*N*^αHis-ac) chelator and evaluated in breast cancer patients.²¹⁶ A clear tumor uptake of [^{99m}Tc-*N*^αHis-ac-Lys⁴,Phe⁷,Pro³⁴]-NPY was observed, whereas normal tissues and organs only showed background radiation.²¹⁶

The short NPY analog [Pro³⁰, Nle³¹, Bpa³², Leu³⁴]-NPY(28–36) (NPY1, Table 7),²¹⁷ with high affinity and selectivity for Y1 receptor, was labelled with ^{99m}Tc and ⁶⁷Ga using pzNN and DOTA chelators, respectively.²¹⁸ The biological interest of such radiopeptides has still to be demonstrated. Another short NPY analog, [Pro³⁰, Tyr³², Leu³⁴]-NPY(28–36) (BVD15), conjugated to DOTA at different positions was also described and the affinity to Y1R evaluated.²¹⁹ It has been shown that the introduction of the BFC at the N-terminus of the peptide led to poor affinity, but the conjugate [Lys⁴(DOTA)]-BVD15 (Table 7) and the respective Cu-complex presented good affinity in the MCF-7 breast cancer cell line.²¹⁹

Peptides targeting the melanocortin 1 (MC1) receptor

α-Melanocyte-stimulating hormone (α-MSH), a linear tridecapeptide (Table 8), binds to five subtypes of melanocortin receptors (MC1–MC5).²²⁰ Among these, the melanocortin type 1 receptor (MC1R) is overexpressed in both melanotic and amelanotic murine and human melanoma cells.^{221–223} Furthermore,

Table 8 α-MSH and analogs^a

Amino acid sequence:

Ac-Ser-Tyr-Ser-Met⁴-Glu⁵-His-Phe⁷-Arg-Trp-Gly-Lys-Pro-Val-NH₂ (**α-MSH**)
 Ac-Ser-Tyr-Ser-Nle⁴-Glu⁵-His-**dPhe**⁷-Arg-Trp-Gly-Lys-Pro-Val-NH₂ (**NDP-MSH**)
 Ac-Nle⁴-Asp⁵-His-**dPhe**⁷-Arg-Trp-Gly-Lys-NH₂ (**NAPamide**)
 Ac-Cys³-Cys⁴-Glu⁵-His-**dPhe**⁷-Arg-Trp-Cys¹⁰-Lys-Pro-Val-NH₂ (**CCMSH**)
 Ac-Cys³-Cys⁴-Glu⁵-His-**dPhe**⁷-Arg-Trp-Cys¹⁰-Arg¹¹-Pro-Val-NH₂ (**CCMSH(Arg¹¹)**)
 Ac-cyclo[Cys⁴-Glu⁵-His-**dPhe**⁷-Arg-Trp-Cys¹⁰]-Lys-Pro-Val-NH₂ (**CMSH**)
 Ac-Nle⁴-cyclo[Asp⁵-His-**dPhe**⁷-Arg-Trp-Lys¹⁰]-NH₂ (**Melanotan-II: MTII**)
 βAla³-Nle⁴-cyclo[Asp⁵-His-**dPhe**⁷-Arg-Trp-Lys¹⁰]-NH₂ (**βAlaMT-II**)
 βAla³-Nle⁴-Asp⁵-His-**dPhe**⁷-Arg-Trp-Lys¹⁰-NH₂ (**MSHoct**)

^a Amino acid residues in bold type are important for the biological activity of the peptide.

more than 80% of human metastatic melanoma samples have also been identified to display MC1R receptors. Thus, MC1R became a potential target for the diagnosis and therapy of melanoma and metastases, and several linear and cyclic radiolabeled α-MSH analogs have been studied as candidates for MC1R targeting (Table 8).^{5,18,224,225} Structure–bioactivity studies have shown that the minimal sequence of α-MSH required for biological activity is His-Phe-Arg-Trp, and that the replacement in α-MSH of Met⁴ and Phe⁷ by Nle and dPhe, respectively, leads to the potent [Nle⁴,dPhe⁷]-αMSH analog (NDP-MSH, IC₅₀ = 0.21 nM), which is enzymatically stable and has a long half-life.²²⁰

The peptide NDP-MSH was radiolabeled with ^{99m}Tc and ¹⁸⁸Re using as BFCs mercapto-acetylglucylglycine (MAG₂) or the tetrapeptide Ac-Cys-Gly-Cys-Gly (CGCG).²²⁶ The short linear peptide [βAla³,Nle⁴,Asp⁵,dPhe⁷,Lys¹⁰]-αMSH(3–10) (MSHoct) was conjugated to DOTA and to pzNN through the N-terminus and labeled with ¹¹¹In and ^{99m}Tc, respectively.^{227,228} Despite the improved potency of NDP-MSH and MSHoct analogs, the resulting radiolabeled peptides have shown poor *in vivo* behavior. Another analog, [Ac-Nle⁴,Asp⁵,dPhe⁷]-αMSH(4–11) (NAPamide), with high affinity for MC1R, was also conjugated to DOTA and to pzNN through the lateral chain of Lys¹¹. The DOTA derivative was labeled with ¹¹¹In, ⁶⁸Ga and ⁶⁴Cu, while the pzNN-conjugate was labeled with ^{99m}Tc.^{229–231} *In vivo* evaluation has shown that the ⁶⁴Cu-labeled peptide was unstable, with high liver and kidney uptake. The other labeled peptides were stable *in vivo* but have shown only a moderate tumor uptake.

To reduce kidney reabsorption, several glycosylated derivatives of NAPamide were conjugated to DOTA and labeled with ¹¹¹In. *In vivo* studies (B16F1-melanoma mice) confirmed the improvement of pharmacokinetics but the tumor uptake and retention was relatively low.²³²

Several homobivalent NAPamide derivatives containing DOTA or pzNN were labeled with ¹¹¹In and with the tricarbonyl core, respectively.^{233,234} In the case of ¹¹¹In, the dimeric peptides displayed excellent receptor affinity and internalization, but the tumor uptake was low and the kidney accumulation high, compared to the monomeric ¹¹¹In-DOTA-NAPamide.²³⁴

Cyclized α-MSH analogs have also been used to improve binding affinity, *in vivo* stability, and receptor selectivity. Among

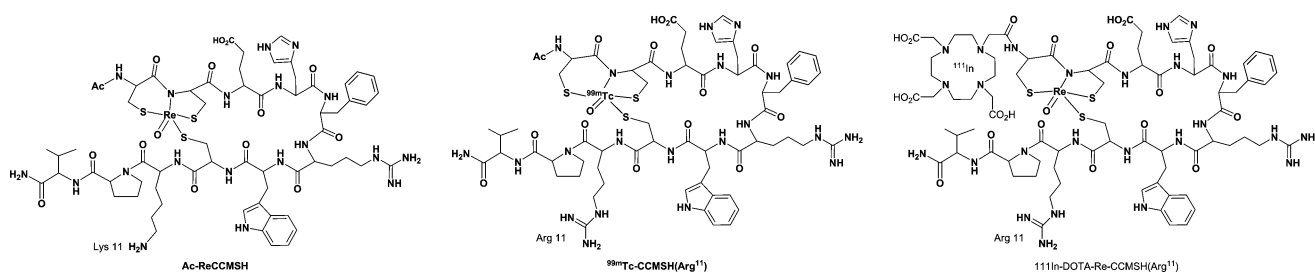


Fig. 11 Structures of Ac-ReCCMSH, ^{99m}Tc-CCMSH(Arg¹¹), and ¹¹¹In-DOTA-Re-CCMSH(Arg¹¹).

cyclization strategies, the disulfide-, lactam- and metal-based cyclizations have been the most explored.^{5,18,224} The peptide [Cys^{4,10},DPh^{e7}]α-MSH (CCMSH), cyclized *via* a disulfide bond, was conjugated to DOTA and labeled with ¹¹¹In. *In vivo* evaluation of the resulting radiopeptide ¹¹¹In-DOTA-CCMSH has shown moderate tumor uptake and high kidney accumulation.²³⁵ Another approach consisted of the cyclization of an α-MSH analog through site-specific rhenium (Re) and technetium (Tc) metal coordination. Such cyclic analogs were structurally characterized and their ability to bind melanoma cells evaluated.²³⁶ It was found that the metal promotes cyclization by coordination to Cys^{3,4,10} sulfhydryls and to Cys⁴ amide nitrogen (Fig. 11). The resulting Re-peptide complex Re-[Cys^{3,4,10},DPh^{e7}]α-MSH(3–13) (ReCCMSH), displayed a high receptor-binding affinity. The corresponding ^{99m}Tc complex ^{99m}Tc-CCMSH, although having high kidney uptake, successfully targeted B16F1-melanoma becoming the proof-of-principle for the potential use of metal-cyclized radiolabeled compounds for melanoma imaging or therapy.²³⁶ Another interesting approach was the conjugation of the metal-cyclized complex Re-CCMSH to DOTA, followed by labelling with ¹¹¹In.²³⁵ Compared to the linear analog ¹¹¹In-DOTA-CCMSH, the Re-cyclized radiopeptide ¹¹¹In-DOTA-Re-CCMSH presented increased tumor-targeting capacity, higher tumor retention and enhanced renal clearance in murine melanoma-bearing mice.²³⁵ By comparing the two metal-based cyclized CCMSH analogs, ¹¹¹In-DOTA-Re-CCMSH *versus* ^{99m}Tc-CCMSH, similar tumor uptake was found, but the Re-mediated cyclized radiopeptide had an enhanced whole-body clearance and a higher tumor-to-blood ratio.²³⁷ Despite the favorable features of ¹¹¹In-DOTA-Re-CCMSH, a relatively high level of radioactivity still remained in the kidneys. Aiming to reduce kidney retention, four new ¹¹¹In-DOTA-derivatized Re-CCMSH analogs were designed, and the analog ¹¹¹In-DOTA-Re-CCMSH(Arg¹¹) (Lys¹¹ replaced by Arg, Fig. 11) showed the highest tumor uptake and the lowest kidney radioactivity accumulation in a murine melanoma model.²³⁸ The analog CCMSH(Arg¹¹) was also cyclized through labelling with ^{99m}Tc (Fig. 11).²³⁹ Also in this case, the replacement of Lys¹¹ by Arg improved tumor uptake and reduced kidney accumulation. Compared to the Re-cyclized analog ¹¹¹In-DOTA-Re-CCMSH(Arg¹¹), ^{99m}Tc-CCMSH(Arg¹¹) exhibited favorable and comparable tumor-targeting properties, and both allowed clear micro-SPECT/CT images of flank melanoma tumors as well as of B16F10 pulmonary melanoma metastases, with ^{99m}Tc-CCMSH(Arg¹¹) providing images with greater resolution of metastatic lesions.²³⁹

These promising properties prompted the direct labeling of the linear peptide CCMSH(Arg¹¹) with ¹⁸⁸Re, yielding the complex ¹⁸⁸Re-CCMSH(Arg¹¹).^{240,241} Its therapeutic efficacy was assessed in

C57BL6 mice bearing B16/F1 murine melanoma tumors and in TXM-13 human melanoma xenografted SCID mice.²⁴² In both, the therapeutic effect of ¹⁸⁸Re-CCMSH(Arg¹¹) on tumor growth was dose-dependent.

For PET imaging of MC1R, the DOTA-Re-CCMSH(Arg¹¹) conjugate was labeled with ⁶⁴Cu and ⁸⁶Y.²⁴³ Complex ⁶⁴Cu-DOTA-Re-CCMSH(Arg¹¹) had high radioactivity accumulation in non-target organs, due most likely to the *in vivo* instability of the complex and consequent release of ⁶⁴Cu. To avoid such behaviour, the DOTA chelator was replaced by CBTE2A.²⁴⁴ The *in vitro* MC1R-binding properties of CBTE2A-Re-CCMSH(Arg¹¹) were unchanged relative to DOTA-Re-CCMSH(Arg¹¹).²⁴⁴ Furthermore, the complex ⁶⁴Cu-CBTE2A-Re-CCMSH(Arg¹¹) presented a B16F1-melanoma uptake comparable to ⁶⁴Cu-DOTA-Re-CCMSH(Arg¹¹) but a significantly higher ratios of tumor to non-target tissues. *In vivo* studies have also shown that ⁶⁴Cu-CBTE2A-Re-CCMSH(Arg¹¹) provided better PET images than ⁸⁶Y-DOTA-Re-CCMSH(Arg¹¹), due to increased tumor retention and kidney clearance.

Still for PET, ⁶⁸Ga-DOTA-Re-CCMSH(Arg¹¹) of low and high specific activity was prepared and evaluated.^{245,246} Despite some differences in the biological profile, in both cases the tumor uptake was low compared to the linear α-MSH analog ⁶⁸Ga-DOTA-NAPamide in the same melanoma animal model. Such results indicated that the Re-mediated cyclization did not bring significant advantages when the radiometal is ⁶⁸Ga. To evaluate the therapeutic potential of these cyclic peptides, ¹⁷⁷Lu-DOTA-Re-CCMSH(Arg¹¹) was prepared. Its *in vivo* evaluation showed a high and prolonged tumor uptake, but also high non-specific kidney accumulation.^{247,248} The tumor growth rate of treated mice was substantially reduced. The authors have also studied the same peptide conjugate labeled with ²¹²Pb. They have found dramatic dose-dependent reductions in tumor growth rates for ²¹²Pb-DOTA-Re(Arg¹¹)CCMSH, and postmortem histopathological examination of the tumor and other major organs showed no sign of primary or metastatic melanoma.²⁴⁹ All treated groups displayed a significant improvement in mean survival time with minor kidney damage.²⁴⁹

A heterobivalent complex, ^{99m}Tc-RGD-Lys-CCMSH(Arg¹¹), was synthesized for dual imaging of integrin and MC1 receptor-expressing tumors. Biodistribution studies in B16F1 melanoma-bearing C57BL6 mice have shown a tumor accumulation and retention higher than those found for ^{99m}Tc-CCMSH(Arg¹¹), but an extremely high kidney uptake was observed.²⁵⁰

As an alternative to metal-cyclized α-MSH analogs, a promising cyclization approach based on a side chain lactam-bridge was recently introduced.²²⁴ Using the potent lactam-cyclized

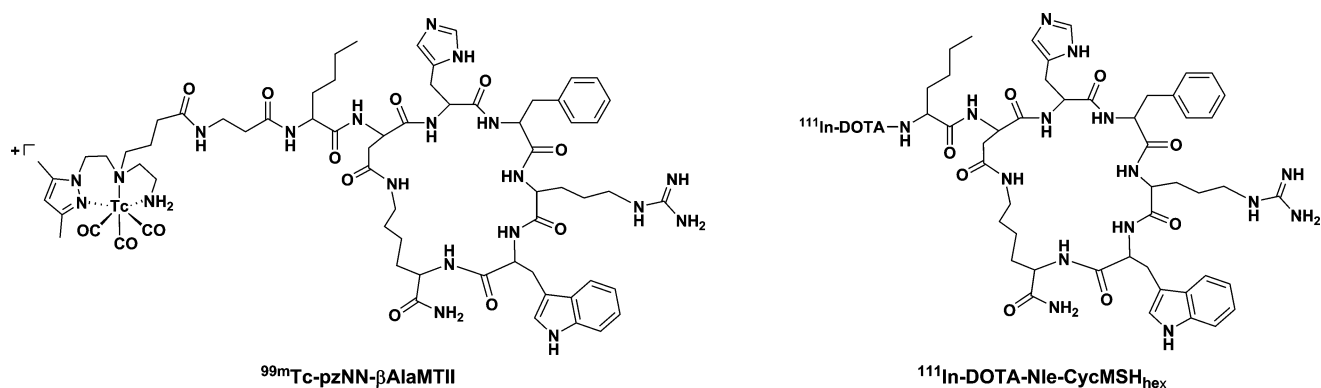


Fig. 12 Structures of $^{99m}\text{Tc-pzNN-}\beta\text{AlaMT-II}$ and $^{111}\text{In-DOTA-Nle-CycMSH}_{\text{hex}}$.

agonist Melanotan II (MT-II) as model, the cyclic peptide $\beta\text{Ala-Nle-c[Asp-His-DPhe-Arg-Trp-Lys]-NH}_2$ ($\beta\text{AlaMT-II}$) was synthesized, conjugated to the pzNN chelator, and labeled with $\text{fac-}[^{99m}\text{Tc}(\text{CO})_3]^+$ (Fig. 12).^{228,251} The radiometallated peptide $^{99m}\text{Tc}(\text{CO})_3\text{-pzNN-}\beta\text{AlaMT-II}$ had high binding affinity and a remarkable internalization in B16F1 cells when compared with its linear analog and with the metal-cyclized $^{99m}\text{Tc-CCMSH}$.^{228,252} In B16F1 melanoma-bearing mice, $^{99m}\text{Tc}(\text{CO})_3\text{-pzNN-}\beta\text{AlaMT-II}$ has also showed a significant MC1R-mediated tumor uptake comparable to that obtained for metal-based cyclic peptides $^{99m}\text{Tc-CCMSH}$ and $^{99m}\text{Tc-CCMSH}(\text{Arg}^{11})$.^{236,238}

Longer lactam-based cyclic α -MSH analogs, CycMSH and GlyGlu-CycMSH (12-amino acid ring), were conjugated to DOTA, through the peptide N-terminal, and labeled with ^{111}In .²⁵³ Both radiopeptides exhibited high receptor-mediated tumor uptake in B16F1 melanoma-bearing mice. These values were comparable to those found for the lactam-based cyclic $^{99m}\text{Tc-pzNN-}\beta\text{AlaMT-II}$ and for the metal-cyclized $^{111}\text{In-DOTA-Re-CCMSH}$, but lower than those found for $^{111}\text{In-DOTA-Re-CCMSH}(\text{Arg}^{11})$. The introduction of GlyGlu in the CycMSH sequence has reduced kidney accumulation.

These results have prompted the synthesis of $^{67}\text{Ga-DOTA-GlyGlu-CycMSH}$ and its biological assessment in B16/F1 melanoma-bearing mice. Kidney accumulation higher than tumor uptake was observed, but both flank primary B16/F1 melanoma and B16/F10 pulmonary melanoma metastases could be clearly visualized by SPECT/CT imaging.²⁵⁴

To evaluate the effect of DOTA position in the peptide backbone, GlyGlu-CycMSH was acetylated in the N-terminus, conjugated to DOTA through the Lys in the cyclic ring, and labeled with ^{111}In . The overall pharmacokinetic profile of the resulting radiopeptide did not improve.²⁵⁵ The same authors also evaluated the effect of the ring size on biodistribution.²⁵⁶ Thus, DOTA was conjugated to the N-terminus of MT-II (6-amino acid peptide ring) and labeled with ^{111}In (Fig. 12). The resulting radiopeptide, $^{111}\text{In-DOTA-Nle-CycMSH}_{\text{hex}}$ presented a rapid and high tumor uptake, a prolonged tumor retention and a moderate kidney accumulation. When compared to $^{111}\text{In-DOTA-GlyGlu-CycMSH}$ with a 12-amino acid ring, the reduction of the peptide ring size dramatically increased the melanoma uptake and decreased the renal retention.^{253,256} The tumor-targeting properties and pharmacokinetics of $^{111}\text{In-DOTA-Nle-CycMSH}_{\text{hex}}$ were more favorable than those presented by the first lactam-cyclized 6-amino

Table 9 Neurotensin and analogs^a

Amino acid sequence:

$p\text{Glu-Leu-Tyr-Glu-Asn-Lys-Pro-Arg-Arg-Pro-Tyr-Ile-Leu-OH}$ (NT)
 $\text{H-Arg-Arg-Pro-Tyr-Ile-Leu-OH}$ (NT(8-13))
 $\text{Lys-}\psi(\text{CH}_2\text{-NH})\text{-Arg-Pro-Tyr-Ile-Leu-OH}$ (NT-VI)
 $\text{Lys-}\psi(\text{CH}_2\text{-NH})\text{-Arg-Pro-Tyr-Tle-Leu-OH}$ (NT-XI)
 $\text{Ahx-Arg-Me-Arg-Pro-Tyr-Tle-Leu-OH}$ (NT-XII)
 $\text{Arg-Me-Arg-Pro-Dmt-Tle-Leu-OH}$ (NT-XIX)
 $\text{Ac-Lys-Pro-Me-Arg-Arg-Pro-Tyr-Tle-Leu-OH}$ (NT-20.3)

^a Amino acid residues in bold type are important for the biological activity of the peptide.

acid ring radiopeptide $^{99m}\text{Tc-pzNN-}\beta\text{AlaMT-II}$.^{228,256} Finally, the lactam-cyclized $^{111}\text{In-DOTA-Nle-CycMSH}_{\text{hex}}$ displayed a tumor-to-kidney ratio comparable to the best metal-cyclized radiopeptide $^{111}\text{In-DOTA-Re-CCMSH}(\text{Arg}^{11})$, suggesting a high potential of lactam-based cyclic radiolabeled α -MSH analogs for MC1R-melanoma targeting.

Peptides targeting the neurotensin (NT) receptor

Neurotensin (NT) is a 13 amino acid peptide (Table 9) that binds to three NT receptor subtypes (NTS1-NTS3). Most NT biological effects are mediated by NTS1, and NT(8–13) is the minimal sequence that mimics the effects of full-length NT.²⁵⁷ Overexpression of NT receptors has been found in many tumors, namely Ewing's sarcoma, meningiomas, SCLC, MTC, ductal pancreatic adenocarcinomas (>70% overexpression) and invasive ductal breast cancers.^{258–261} Numerous NT(8–13) analogues (Table 9) containing the (N α His)Ac chelator and labeled with ^{99m}Tc or ^{188}Re have been synthesized.^{262–268} Among all the radiometallated neurotensin analogs, [$^{99m}\text{Tc}(\text{CO})_3\text{-(N}^\alpha\text{His)Ac-NT-XIX}$] displayed the highest tumor uptake with low accumulation in non-target organs, particularly in kidneys.^{265,266} Encouraging therapeutic effects were also obtained in nude mice injected with the ^{188}Re -analogue.²⁶⁵

NTS1-binding NT analogs conjugated to DTPA or DOTA chelators have been synthesized and labeled with ^{111}In .²⁶⁹ These radiopeptides had unfavorable ratios of tumor to non-target organs. In order to increase tumor uptake and reduce kidney accumulation, two novel families of DTPA-NT analogs have been proposed. The first family comprises a series of DTPA-NT(8–13) analogs (DTPA-NT-VI, DTPA-NT-XI, DTPA-Ahx-NT-XII and

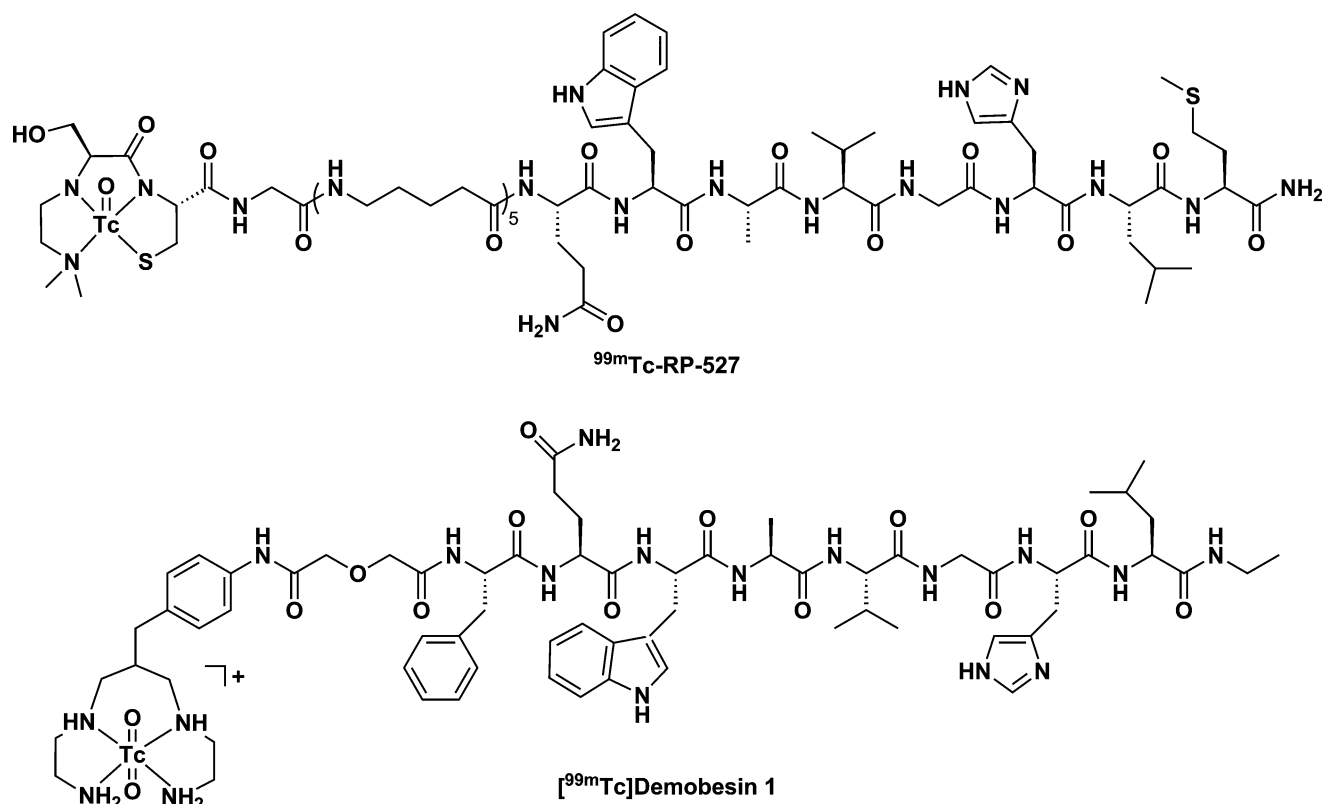


Fig. 13 Structures of ^{99m}TcO -RP-527 and $^{99m}\text{TcO}_2$ -demobesin 1.

DTPA-Ahx-NT-XIX), which share the same peptide sequence with the analogs bearing the ($N\alpha$ -His)Ac moiety described previously. The second series of DTPA-peptides are analogs of NT(6–13) peptide (Table 9), in which DTPA was coupled to the ϵ - NH_2 of Lys⁶.²⁷⁰ Structure activity studies demonstrated that the attachment of DTPA induces an important loss of affinity, unless the distance between the BFCA and the biologically active sequence (NT(8–13)) is increased. Among all the radiopeptides, ^{111}In -DTPA-NT-20.3 was the most promising, with high tumor uptake but still with a high kidney accumulation. In spite of the kidney retention, the tumor-to-intestine ratio was higher than that found for $[^{99m}\text{Tc}(\text{CO})_3\text{-(}N\alpha\text{His)Ac-NT-XIX}]$.

Radiopeptides targeting the gastrin-releasing peptide (GRP) receptor

Bombesin (BBN, $p\text{Glu}^1\text{-Gln}^2\text{-Arg}^3\text{-Leu}^4\text{-Gly}^5\text{-Asn}^6\text{-Gln}^7\text{-Trp}^8\text{-Ala}^9\text{-Val}^{10}\text{-Gly}^{11}\text{-Hist}^{12}\text{-Leu}^{13}\text{-Met}^{14}\text{-NH}_2$) is an amphibian homologue of mammalian gastrin-releasing peptide (GRP) that has very high affinity and specificity for the GRP receptor (GRPr).²⁷¹ To date, four different GRPr subtypes have been characterized, and overexpression of GRPrs has been observed on a variety of tumors including breast, prostate, pancreatic, and small-cell lung cancer (SCLC).² The C-terminal 7–14 amino acid sequence of BBN is essential for high-affinity binding to GRPr. Therefore, various BBN analogs based on the BBN[7–14] NH_2 agonist have been used by many research groups to design radiometallated peptides suitable for diagnostic and therapeutic of GRPr-positive tumors.

Profiting from the diversified chemistry of technetium, different strategies have been used for labeling BBN derivatives with this radiometal. Such strategies involved the use of Tc-HYNIC , $[\text{TcO}]^{3+}$, $\text{trans-}[\text{TcO}_2]^+$, $\text{fac-}[\text{Tc}(\text{CO})_3]^+$ and the Tc(III) '4 + 1' approach, in combination with a variety of bifunctional chelators.^{272–290} The pre-clinical evaluation of these ^{99m}Tc -labelled BBN derivatives led to some encouraging results, but only a few have been tested in the clinic. The radiopeptide ^{99m}Tc -RP-527 (Fig. 13), containing a N_3S chelator coupled to BBN[7–14] via a Gly-5-aminovaleic acid, was able to identify primary breast cancer and prostate cancer and their metastases.²⁷² A more recent achievement has been the introduction of ^{99m}Tc -Demobesin 1 ($[^{99m}\text{Tc-N}_4\text{-DPh}^6\text{,Leu-NHET}_3\text{,des-Met}^{14}\text{]-BBN}^{6-14}$), which contains a TcO_2^+ core and a linear tetraamine as BFC (Fig. 13). ^{99m}Tc -Demobesin 1 exhibited the highest absolute tumor uptake described in the literature for a PC3 xenograft model, while showing a high stability *in vivo* and a favourable pharmacokinetic profile.^{275,287} This radiopeptide has an antagonist character and does not internalize significantly into PC-3 cells, which suggests a change of paradigm on the diagnostic and PRRT of GRPr-positive tumors.

The BBN[7–14] NH_2 analog has been labeled with ^{64}Cu using DOTA, CB-TE2A and NOTA-derivatives and different linkers to modulate pharmacokinetics.^{57,291–300} The resulting radioconjugates behave as agonists and were able to target GRPr-positive xenografted human tumors in a specific way. Due to a prolonged retention of radioactivity in kidneys and gastrointestinal tract, the ^{64}Cu -BBN-DOTA derivatives have showed less favourable target–non-target ratios compared to the radioconjugates-CB-TE2A and NOTA.⁵⁷ These differences have been considered to reflect the

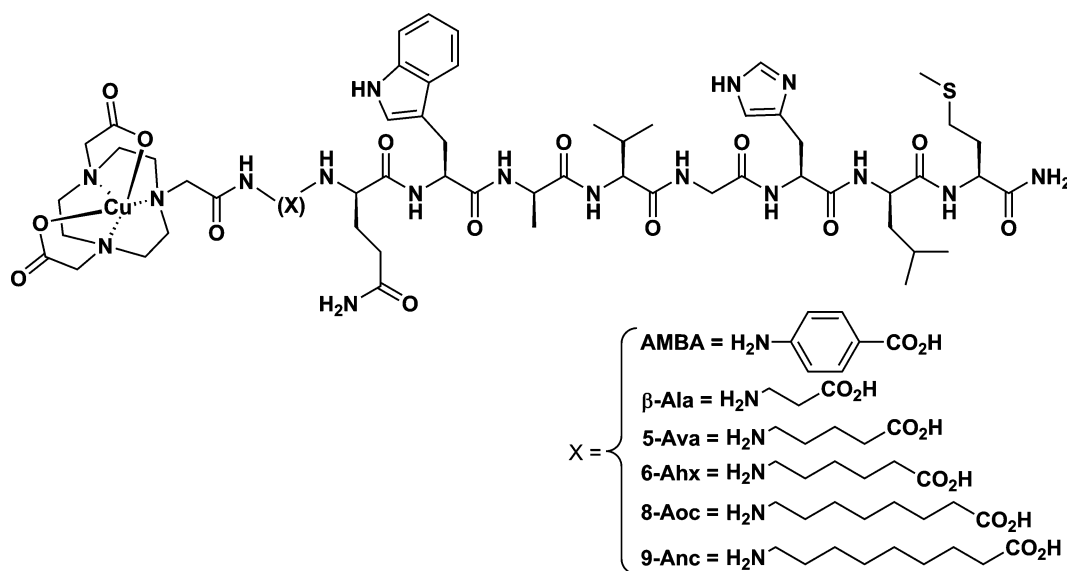


Fig. 14 Chemical structure of $[^{64}\text{Cu-NO}_2\text{A-(X)-BBN[7-14]}$.

highest *in vivo* stability of Cu(II) complexes with CB-TE2A and NOTA chelators. The most promising results were reported by Smith and co-workers for the radiopeptide $[^{64}\text{Cu-NO}_2\text{A-(X)-BBN[7-14]}$, where NO₂A (1,4,7-triazacyclononane-1,4-diacetic acid) is a NOTA derivative and X are pharmacokinetic modifiers (Fig. 14). The radiopeptide $[^{64}\text{Cu-NO}_2\text{A-(AMBA)-BBN[7-14]}$, containing the shorter and more hydrophilic linker, exhibited the highest tumor accumulation and the fastest clearance from non-target tissues, emerging as a good candidate for further evaluation in humans.³⁰⁰

Several BBN derivatives were also labeled with the trivalent radiometals $^{67/68}\text{Ga}$, ^{111}In and ^{177}Lu , using DOTA-like chelators and different linkers to improve the pharmacokinetics.³⁰¹⁻³¹⁴ Two of these derivatives, $^{68}\text{Ga-DOTABOM}$ and $^{177}\text{Lu-AMBA}$, underwent clinical trials for PET detection or PRRT of prostate cancer (PC), respectively. $^{68}\text{Ga-DOTABOM}$ allowed the detection of malignant PC lesions in 13 out of 15 patients.³⁰¹ Within a phase I study and aiming at PC therapy, $^{177}\text{Lu-AMBA}$ ($^{177}\text{Lu-DOTA-G-4-aminobenzyl-BBN}^{7-14}$) detected lesions in 5 out of 7 patients.³¹¹

Concluding remarks and perspectives

Peptide-based nuclear tools for molecular imaging and therapy have now become an established approach, mainly due to the success achieved with somatostatin analogs, increasing knowledge into the cell and molecular biology of malignancies, advances in the coordination chemistry of radiometals, and bioconjugation. Numerous radiometallated peptides to target receptors over-expressed in tumor cells have been synthesized and their biological properties studied and correlated with chemical structures. However, most of those metal complexes have been evaluated only in animal models, still being under investigations that aim to optimize *in vivo* stability, target-affinity and target–non-target ratios. The advantages of using homo- or heteromultimeric radiometallated peptides based on agonists or antagonists must still be addressed in the future.

Acknowledgements

The Fundação para a Ciência e Tecnologia (FCT) is acknowledged for financial support (POCI/SAU-FCF/58855/2004 and PTDC/QUI-QUI/115712/2009).

References

- 1 World Health Organization Fact Sheet no. 297 – Cancer, 2009.
- 2 J. C. Reubi, *Endocr. Rev.*, 2003, **24**, 389–427.
- 3 H.-J. Wester, *Clin. Cancer Res.*, 2007, **13**, 3470–3481.
- 4 R. von der Meel, W. M. Gallagher, S. Oliveira, A. E. O'Connor, R. Schifferles and A. T. Byrne, *Drug Discovery Today*, 2010, **15**, 102–114.
- 5 M. Schottellius and H.-J. Wester, *Methods*, 2009, **48**, 161–177.
- 6 M. F. Tweedle, *Acc. Chem. Res.*, 2009, **42**, 958–968.
- 7 J. C. Reubi and H. R. Maecke, *J. Nucl. Med.*, 2008, **49**, 1735–1738.
- 8 *Targeted Radionuclide Tumor Therapy Biological Aspects*, ed. T. Stigbrand, J. Carlsson and G. P. Adams, Springer Science, 2008.
- 9 *Monoclonal Antibody and Peptide-Targeted Radiotherapy of Cancer*, ed. R. M. Reilly, J. Wiley & Sons, 1st edn, 2010.
- 10 T. Olafsen and A. M. Wu, *Semin. Nucl. Med.*, 2010, **40**, 167–181.
- 11 S. E. Pool, E. P. Krenning, G. A. Koning, C. H. J. van Eijck, J. J. M. Teunissen, B. Kam, R. Valkema, D. J. Kwekkeboom and M. de Jong, *Semin. Nucl. Med.*, 2010, **40**, 209–218.
- 12 L. Bodei, D. Ferone, C. M. Grana, M. Cremonesi, A. Signore, R. A. Dierckx and G. Paganelli, *J. Endocrinol. Invest.*, 2009, **32**, 360–369.
- 13 M. van Essen, E. P. Krenning, B. L. R. Kam, M. de Jong, R. Valkema and D. J. Kwekkeboom, *Nat. Rev. Endocrinol.*, 2009, **5**, 382–393.
- 14 M. De Jong, W. A. P. Breeman, D. J. Kwekkeboom, R. Valkema and E. P. Krenning, *Acc. Chem. Res.*, 2009, **42**, 873–880.
- 15 E. Bombardieri, A. Coliva, M. Maccauro, E. Seregni, E. Orunesu, A. Chiti and G. Lucignani, *Q. J. Nucl. Med. Mol. Imaging*, 2010, **54**, 3–15.
- 16 D. J. Kwekkeboom, W. W. de Herder, C. H. J. van Eijck, B. L. Kam, M. van Essen, J. J. M. Teunissen and E. P. Krenning, *Semin. Nucl. Med.*, 2010, **40**, 78–88.
- 17 D. J. Kwekkeboom, B. L. Kam, M. van Essen, J. J. M. Teunissen, C. H. J. van Eijck, R. Valkema, M. De Jong, W. W. de Herder and E. P. Krenning, *Endocr. Relat. Cancer*, 2010, **17**, R53–R73.
- 18 S. Lee, J. Kie and X. Chen, *Chem. Rev.*, 2010, **110**, 3087–3111.
- 19 S. Roosenburg, P. Laverman, F. L. van Delft and O. C. Boerman, *Amino Acids*, 2010, DOI: 10.1007/s00726-010-0501-y.
- 20 S. Liu and D. S. Edwards, *Bioconjugate Chem.*, 2001, **12**, 7–34.
- 21 M. Shokeen and C. J. Anderson, *Acc. Chem. Res.*, 2009, **42**, 832–841.
- 22 R. E. Mewis and S. J. Archibald, *Coord. Chem. Rev.*, 2010, **254**, 1686–1712.

- 101 R. Haubner, A. J. Beer, H. Wang and X. Chen, *Eur. J. Nucl. Med. Mol. Imaging*, 2010, **37**(S1), 86–S103.
- 102 L. W. Dobrucki, E. D. de Muinck, J. R. Lindner and A. J. Sinusas, *J. Nucl. Med.*, 2010, **51**, 66S–79S.
- 103 R. Haubner, H.-J. Wester, W. A. Weber, C. Mang, S. I. Ziegler, S. L. Goodman, R. Senekowitsch-Schmidtke, H. Kessler and M. Schwaiger, *Cancer Res.*, 2001, **61**, 1781–1785.
- 104 R. Haubner, R. Gratias, B. Diefenbach, S. L. Goodman, A. Jonczyk and H. Kessler, *J. Am. Chem. Soc.*, 1996, **118**, 7461–7472.
- 105 K. E. Gottschalk and H. Kessler, *Angew. Chem., Int. Ed.*, 2002, **41**, 3767–3774.
- 106 S. Liu, E. Cheung, M. C. Ziegler, M. Rajopadhye and D. S. Edwards, *Bioconjugate Chem.*, 2001, **12**, 559–568.
- 107 M. Janssen, W. J. G. Oyen, L. F. A. G. Massuger, C. Frielink, I. Dijkgraaf, D. S. Edwards, M. Radjopadhye, F. H. M. Corstens and O. C. Boerman, *Cancer Biother. Radiopharm.*, 2002, **17**, 641–646.
- 108 S. Liu, D. S. Edwards, M. C. Ziegler, A. R. Harris, S. J. Hemingway and John A. Barrett, *Bioconjugate Chem.*, 2001, **12**, 624–629.
- 109 Y. Wu, X. Zhang, Z. Xiong, Z. Cheng, D. R. Fisher, S. Liu, S. S. Gambhir and X. Chen, *J. Nucl. Med.*, 2005, **46**, 1707–1718.
- 110 I. Dijkgraaf, S. Liu, J. A. W. Kruijtzter, A. C. Soede, W. J. G. Oyen, R. M. J. Liskamp, F. H. M. Corstens and O. C. Boerman, *Nucl. Med. Biol.*, 2007, **34**, 29–35.
- 111 I. Dijkgraaf, J. A. W. Kruijtzter, S. Liu, A. Soede, W. J. G. Oyen, F. H. M. Corstens, R. M. J. Liskamp and O. C. Boerman, *Eur. J. Nucl. Med. Mol. Imaging*, 2007, **34**, 267–273.
- 112 S. Liu, Y. S. Kim, W. Y. Hsieh and S. G. Sreerama, *Nucl. Med. Biol.*, 2008, **35**, 111–121.
- 113 B. Jia, Z. Liu, J. Shi, Z. L. Yu, Z. Yang, H. Y. Zhao, Z. J. He, S. Liu and F. Wang, *Bioconjugate Chem.*, 2008, **19**, 201–210.
- 114 J. J. Wang, Y. S. Kim, Z. J. He and S. Liu, *Bioconjugate Chem.*, 2008, **19**, 634–642.
- 115 Z. Li, W. Cai, Q. Cao, K. Chen, Z. Wu and X. Chen, *J. Nucl. Med.*, 2007, **48**, 1162–1171.
- 116 D. Boturyn, J.-L. Coll, E. Garanger, M.-C. Favrot and P. Dumy, *J. Am. Chem. Soc.*, 2004, **126**, 5730–5739.
- 117 C. Wängler, S. Maschauer, O. Prante, M. Schäfer, R. Schirrmacher, P. Bartenstein, M. Eisenhut and B. Wängler, *ChemBioChem*, 2010, **11**, 2168–2181.
- 118 E. Noiri, M. S. Goligorsky, G. J. Wang, J. Wang, C. J. Cabahug, S. Sharma, B. A. Rhodes and P. Som, *J. Am. Soc. Nephrol.*, 1996, **7**, 2682–2688.
- 119 G. B. Sivolapenko, D. Skarlos, D. Pectasides, E. Stathopoulou, A. Milonakis, G. Sirmalis, A. Stuttle, N. S. Courtenay-Luck, K. Konstantinides and A. A. Epenetos, *Eur. J. Nucl. Med. Mol. Imaging*, 1998, **25**, 1383–1389.
- 120 D. Edwards, P. Jones, H. Haramis, M. Battle, R. Lear, D. J. Barnett, C. Edwards, H. Crawford, A. Black and V. Godden, *Nucl. Med. Biol.*, 2008, **35**, 365–375.
- 121 T. Bach-Gansmo *et al.*, *J. Nucl. Med.*, 2006, **47**, 1434–1439.
- 122 R. Axelsson, T. Bach-Gansmo, J. Castell-Conesa and B. J. McParland, *Acta Radiol.*, 2010, **51**, 40–46.
- 123 M. L. Janssen, W. J. Oyen, I. Dijkgraaf, L. F. Massuger, C. Frielink, D. S. Edwards, M. Rajopadhye, H. Boonstra, F. H. Corstens and O. C. Boerman, *Cancer Res.*, 2002, **62**, 6146–6151.
- 124 S. Liu, W. Y. Hsieh, Y. S. Kim and S. I. Mohammed, *Bioconjugate Chem.*, 2005, **16**, 1580–1588.
- 125 L. Wang *et al.*, *Mol. Pharmaceutics*, 2009, **6**, 231–45.
- 126 J. Shi *et al.*, *J. Med. Chem.*, 2008, **51**, 7980–90.
- 127 M. Fani, D. Psimadas, C. Zikos, S. Xanthopoulos, G. K. Loudos, P. Bouziotis and A. D. Varvarigou, *Anticancer Res.*, 2006, **26**, 431–434.
- 128 K. H. Jung, K. H. Lee, J. Y. Paik, B. H. Ko, J. S. Bae, B. C. Lee, H. J. Sung, D. H. Kim, Y. S. Choe and D. Y. Chi, *J. Nucl. Med.*, 2006, **47**, 2000–2007.
- 129 C. Decristoforo, I. Santos, H. J. Pietzsch, J. U. Kuenstler, A. Duatti, C. J. Smith, A. Rey, R. Alberto, E. Von Guggenberg and R. Haubner, *Q. J. Nucl. Med. Mol. Imaging*, 2007, **51**, 33–41.
- 130 P. M. van Hagen, W. A. Breeman, H. F. Bernard, M. Schaar, C. M. Mooij, A. Srinivasan, M. A. Schmidt, E. P. Krenning and M. de Jong, *Int. J. Cancer*, 2000, **90**, 186–198.
- 131 I. Dijkgraaf, J. A. Kruijtzter, C. Frielink, A. C. Soede, H. W. Hilbers, W. J. Oyen, F. H. Corstens, R. M. Liskamp and O. C. Boerman, *Nucl. Med. Biol.*, 2006, **33**, 953–961.
- 132 X. Chen, Y. Hou, M. Tohme, R. Park, V. Khankaldyyan, I. Gonzales-Gomez, J. R. Bading, W. E. Laug and P. S. Conti, *J. Nucl. Med.*, 2004, **45**, 1776–1783.
- 133 J. Shi, L. Wang, Y. S. Kim, S. Zhai, Z. Liu, X. Chen and S. Liu, *Bioconjugate Chem.*, 2009, **20**, 750–759.
- 134 Z. Liu, G. Niu, J. Shi, S. L. Liu, F. Wang, S. Liu and X. Chen, *Eur. J. Nucl. Med. Mol. Imaging*, 2009, **36**, 947–957.
- 135 J. Shi, Y.-S. Kim, S. Chakraborty, Y. Zhou, F. Wang and S. Liu, *Amino Acids*, 2010, DOI: 10.1007/s00726-009-0439-0.
- 136 S. Chakraborty, J. Shi, Y.-S. Kim, Y. Zhou, B. Jia, F. Wang and S. Liu, *Bioconjugate Chem.*, 2010, **21**, 969–978.
- 137 F. Noble and B. P. Roques, *Prog. Neurobiol.*, 1999, **58**, 349–379.
- 138 F. Noble, S. A. Wank, J. N. Crawley, J. Bradwejn, K. B. Seroogy, M. Hamon and B. P. Roques, *Pharmacol. Rev.*, 1999, **51**, 745–781.
- 139 J. J. Vanderhaeghen, J. C. Signeau and W. Gepts, *Nature*, 1975, **257**, 604–605.
- 140 M. R. Hellmich, X. L. Rui, H. L. Hellmich, R. Y. D. Fleming, B. M. Evers and C. M. Townsend, *J. Biol. Chem.*, 2000, **275**, 32122–32128.
- 141 J. C. Reubi and B. Waser, *Int. J. Cancer*, 1996, **67**, 644–647.
- 142 J. C. Reubi, J. C. Schaer and B. Waser, *Cancer Res.*, 1997, **57**, 1377–1386.
- 143 M. Gotthardt, M. P. Béhé, J. Grass, A. Bauhofer, A. Rinke, M. L. Schipper, M. Kalinowski, R. Arnold, W. J. G. Oyen and T. M. Behr, *Endocr. Relat. Cancer*, 2006, **13**, 1203–1211.
- 144 J. C. Reubi, *Curr. Top. Med. Chem.*, 2007, **7**, 1239–1242.
- 145 T. M. Behr and M. P. Béhé, *Semin. Nucl. Med.*, 2002, **32**, 97–109.
- 146 T. M. Behr, N. Jenner, S. Radetzky, M. P. Béhé, S. Gratz, S. Yücekent, F. Raue and W. Becker, *Eur. J. Nucl. Med. Mol. Imaging*, 1998, **25**, 424–430.
- 147 T. M. Behr, N. Jenner, M. P. Béhé, C. Angerstein, S. Gratz, F. Raue and W. Becker, *J. Nucl. Med.*, 1999, **40**, 1029–1044.
- 148 M. Béhé, W. Becker, M. Gotthardt, C. Angerstein and T. M. Behr, *Eur. J. Nucl. Med. Mol. Imaging*, 2003, **30**, 1140–1146.
- 149 M. P. Béhé and T. M. Behr, *Biopolymers*, 2002, **66**, 399–418.
- 150 M. Gotthardt, M. P. Béhé, D. Beuter, A. Battmann, A. Bauhofer, T. Schurrat, M. Schipper, H. Pollum, W. J. G. Oyen and T. M. Behr, *Eur. J. Nucl. Med. Mol. Imaging*, 2006, **33**, 1273–1279.
- 151 S. Good, M. A. Walter, B. Waser, X. Wang, J. Müller-Brand, M. P. Béhé, J. C. Reubi and H. R. Mäcke, *Eur. J. Nucl. Med. Mol. Imaging*, 2008, **35**, 1868–1877.
- 152 M. P. Béhé, G. Kluge, W. Becker, M. Gotthardt and T. M. Behr, *J. Nucl. Med.*, 2005, **46**, 1012–1015.
- 153 S. J. Mather, A. J. McKenzie, J. K. Sosabowski, T. M. Morris, D. Ellison and S. A. Watson, *J. Nucl. Med.*, 2007, **48**, 615–622.
- 154 J. C. Reubi, B. Waser, J. C. Schaer, U. Laederach, J. Erion, A. Srinivasan, M. Schmidt and J. E. Bugaj, *Eur. J. Nucl. Med. Mol. Imaging*, 1998, **25**, 481–490.
- 155 S. Roosenburg, P. Laverman, L. Joosten, A. Eek, W. J. G. Oyen, M. de Jong, F. P. J. T. Rutjes, F. L. van Delft and O. C. Boerman, *Bioconjugate Chem.*, 2010, **21**, 663–670.
- 156 J. Sosabowski, T. Matzow, J. Foster and S. Mather, *Q. J. Nucl. Med. Mol. Imaging*, 2008, **52**, 13(suppl 1).
- 157 J. K. Sosabowski, T. Matzow, J. M. Foster, C. Finucane, D. Ellison, S. A. Watson and S. J. Mather, *J. Nucl. Med.*, 2009, **50**, 2082–2089.
- 158 B. A. Nock, T. Maina, M. P. Béhé, A. Nikolopoulou, M. Gotthardt, J. S. Schmitt, T. M. Behr and H. R. Mäcke, *J. Nucl. Med.*, 2005, **46**, 1727–1736.
- 159 W. A. P. Breeman, A. C. Fröberg, E. De Blois, A. van Gameren, M. Melis, M. De Jong, T. Maina, B. A. Nock, J. L. Erion, H. R. Mäcke and E. P. Krenning, *Nucl. Med. Biol.*, 2008, **35**, 839–849.
- 160 A. C. Fröberg, M. de Jong, B. A. Nock, W. A. P. Breeman, J. L. Erion, T. Maina, M. Verdijseldonck, W. W. De Herder, A. von der Lugt, P. P. M. Kooij and E. P. Krenning, *Eur. J. Nucl. Med. Mol. Imaging*, 2009, **36**, 1265–1272.
- 161 E. von Guggenberg, H. Dietrich, I. Skvortsova, M. Gabriel, I. J. Virgolini and C. Decristoforo, *Eur. J. Nucl. Med. Mol. Imaging*, 2007, **34**, 1209–1218.
- 162 E. von Guggenberg, W. Sallegger, A. Helbok, M. Ocak, R. King, S. J. Mather and C. Decristoforo, *J. Med. Chem.*, 2009, **52**, 4786–4793.
- 163 R. King, M. B.-U. Surfraz, C. Finucane, S. C. G. Biagini, P. J. Blower and S. J. Mather, *J. Nucl. Med.*, 2009, **50**, 591–598.
- 164 M. de Jong, W. H. Bakker, B. F. Bernard, R. Valkema, D. J. Kwekkeboom, J. C. Reubi, A. Srinivasan, M. Schmidt and E. P. Krenning, *J. Nucl. Med.*, 1999, **40**, 2081–2087.

- 165 L. Aloj, C. Caracò, M. Panico, A. Zannetti, S. Del Vecchio, D. Tesaro, S. De Luca, C. Arra, C. Pedone, G. Morelli and M. Salvatore, *J. Nucl. Med.*, 2004, **45**, 485–494.
- 166 S. Brillouet, S. Dorbes, F. Courbon, C. Picard, J. P. Delord, E. Benoist, M. Poirot, B. M. Voegtli and S. S. Poirot, *Bioorg. Med. Chem.*, 2010, **18**, 5400–5412.
- 167 S. Dorbes, B. M. Voegtli, Y. Coulais, C. Picard, S. S. Poirot, M. Poirot and E. Benoist, *Eur. J. Med. Chem.*, 2010, **45**, 423–429.
- 168 P. Laverman, M. Béhé, W. J. G. Oyen, P. H. G. M. Willems, F. H. M. Corstens, T. M. Behr and O. C. Boerman, *Bioconjugate Chem.*, 2004, **15**, 561–568.
- 169 S. Agostini, C. Bolzati, E. Didonè, M. C. Ceccato, F. Refosco, L. Aloj, C. Arra, M. Aurilio, A. L. Tornesello, D. Tesaro and G. Morelli, *J. Pept. Sci.*, 2007, **13**, 211–219.
- 170 L. D. D'Andrea, I. Testa, M. Panico, R. Di Stasi, C. Caracò, L. Tarallo, C. Arra, A. Barbieri, A. Romanelli and L. Aloj, *Biopolymers*, 2008, **90**, 707–712.
- 171 S. I. Said and V. Mutt, *Science*, 1970, **169**, 1217–1218.
- 172 V. Mutt, *Ann. N. Y. Acad. Sci.*, 1988, **527**, 1–19.
- 173 S. Chakder and S. Rattan, *J. Pharm. Exp. Ther.*, 1993, **266**, 392–329.
- 174 A. J. Harmar, A. Arimura, I. Gozes, L. Journot, M. Laburthe, J. R. Pisegna, S. R. Rawlings, P. Robberecht, S. I. Said, S. P. Sreedharan, S. A. Wank and J. A. Waschek, *Pharmacol. Rev.*, 1998, **50**, 265–270.
- 175 J. C. Reubi, U. Läderach, B. Waser, J.-O. Gebbers, P. Robberecht and J. A. Laissue, *Cancer Res.*, 2000, **60**, 3105–3112.
- 176 V. R. Pallela, M. L. Thakur, S. Chakder and S. Rattan, *J. Nucl. Med.*, 1999, **40**, 352–360.
- 177 M. L. Thakur, C. S. Marcus, S. Saeed, V. Pallela, C. Minami, L. Diggle, H. Le Pham, R. Ahdoot and E. A. Kalinowski, *J. Nucl. Med.*, 2000, **41**, 107–110.
- 178 P. S. Rao, M. L. Thakur, V. Pallela, R. Patti, K. Reddy, H. Li, S. Sharma, H. L. Pham, L. Diggle, C. Minami and C. S. Marcus, *Nucl. Med. Biol.*, 2001, **28**, 445–450.
- 179 M. L. Thakur, M. R. Aruva, J. Garipey, P. Acton, S. Rattan, S. Prasad, E. Wickstrom and A. Alavi, *J. Nucl. Med.*, 2004, **45**, 1381–1389.
- 180 K. Zhang, M. R. Aruva, N. Shanthly, C. A. Cardi, C. A. Patel, S. Rattan, G. Cesarone, E. Wickstrom and M. L. Thakur, *Regul. Pept.*, 2007, **144**, 91–100.
- 181 K. Zhang, M. R. Aruva, N. Shanthly, C. A. Cardi, S. Rattan, C. Patel, C. Kim, P. A. McCue, E. Wickstrom and M. L. Thakur, *J. Nucl. Med.*, 2008, **49**, 112–121.
- 182 M. L. Thakur, D. Devadhas, K. Zhang, R. G. Pestell, C. Wang, P. McCue and E. Wickstrom, *J. Nucl. Med.*, 2010, **51**, 106–111.
- 183 K. Kothari, S. Prasad, A. Korde, A. Mukherjee, A. Mathur, M. Jaggi, M. Venkatesh, A. M. R. Pillai, R. Mukherjee and N. Ramamoorthy, *Appl. Radiat. Isot.*, 2007, **65**, 382–386.
- 184 J. C. Reubi, M. Körner, B. Waser, L. Mazzucchelli and L. Guillou, *Eur. J. Nucl. Med. Mol. Imaging*, 2004, **31**, 803–810.
- 185 K. E. Mayo, L. J. Miller, D. Bataille, S. Dalle, B. Göke, B. Thorens and D. J. Drucker, *Pharmacol. Rev.*, 2003, **55**, 167–194.
- 186 M. Gotthardt, M. Fischer, I. Naehar, J. B. Holz, H. Jungclas, H. W. Fritsch, M. Béhé, B. Göke, K. Joseph and T. M. Behr, *Eur. J. Nucl. Med. Mol. Imaging*, 2002, **29**, 597–606.
- 187 M. Gotthardt, G. Lalyko, J. van Eerd-Vismale, B. Keil, T. Schurrat, M. Hower, P. Laverman, T. M. Behr, O. C. Boerman, B. Göke and M. Béhé, *Regul. Pept.*, 2006, **137**, 162–167.
- 188 D. Wild, M. Béhé, A. Wicki, D. Storch, B. Waser, M. Gotthardt, B. Keil, G. Christofori, J. C. Reubi and H. R. Mäcke, *J. Nucl. Med.*, 2006, **47**, 2025–2033.
- 189 A. Wicki, D. Wild, D. Storch, C. Seemayer, M. Gotthardt, M. Behe, S. Kneifel, M. J. Mihatsch, J. C. Reubi, H. R. Mäcke and G. Christofori, *Clin. Cancer Res.*, 2007, **13**, 3696–3705.
- 190 D. Wild, H. Mäcke, E. Christ, B. Gloor and J. C. Reubi, *N. Engl. J. Med.*, 2008, **359**, 766–768.
- 191 E. Christ, D. Wild, F. Forrer, M. Brändle, R. Sahli, T. Clerici, B. Gloor, F. Martius, H. Mäcke and J. C. Reubi, *J. Clin. Endocrinol. Metab.*, 2009, **94**, 4398–4405.
- 192 D. Wild, A. Wicki, R. Mansi, M. Béhé, B. Keil, P. Bernhardt, G. Christofori, P. J. Ell and H. Mäcke, *J. Nucl. Med.*, 2010, **51**, 1059–1067.
- 193 M. Brom, W. J. G. Oyen, L. Joosten, M. Gotthardt and O. C. Boerman, *Eur. J. Nucl. Med. Mol. Imaging*, 2010, **37**, 1345–1355.
- 194 A. Zlotnik and O. Yoshie, *Immunity*, 2000, **12**, 121–127.
- 195 A. Müller, B. Homey, H. Soto, N. Ge, D. Catron, M. E. Buchanan, T. McClanahan, E. Murphy, W. Yuan, S. N. Wagner, J. Luis Barrera, A. Mohar, E. Verástegui and A. Zlotnik, *Nature*, 2001, **410**, 50–56.
- 196 R. S. Taichman, C. Cooper, E. T. Keller, K. J. Pienta, N. S. Taichman and R. S. McCauley, *Cancer Res.*, 2002, **62**, 1832–1837.
- 197 J. D. Abbott, Y. Huang, D. Liu, R. Hickey, D. S. Krause and F. J. Giordan, *Circulation*, 2004, **110**, 3300–3305.
- 198 A. T. Askari, S. Unzek, Z. B. Popovic, C. K. Goldman, F. Forudi, M. Kiedrowski, A. Rovner, S. G. Ellis, J. D. Thomas, P. E. DiCorleto, E. J. Topol and M. S. Penn, *Lancet*, 2003, **362**, 697–703.
- 199 M. Zhang, N. Mal, M. Kiedrowski, M. Chacko, A. T. Askari, Z. B. Popovic, O. N. Koc and M. S. Penn, *FASEB J.*, 2007, **21**, 3197–3207.
- 200 N. Koglin, M. Anton, A. Hauser, D. Saur, H. Algul, R. Schmid, B. Gansbacher, M. Schwaiger and H. J. Wester, *J. Nucl. Med.*, 2006, **47**Suppl. 1, 505P.
- 201 H. Hanaoka, T. Mukai, H. Tamamura, T. Mori, S. Ishino, K. Ogawa, Y. Iida, R. Doi, N. Fujii and H. Saji, *Nucl. Med. Biol.*, 2006, **33**, 489–494.
- 202 P. Misra, D. Lebeche, H. Ly, M. Schwarzkopf, G. Diaz, R. J. Hajjar, A. D. Schecter and J. V. Frangioni, *J. Nucl. Med.*, 2008, **49**, 963–969.
- 203 K. Tatemoto, *Proc. Natl. Acad. Sci. U. S. A.*, 1982, **79**, 5485–5489.
- 204 T. Pedrazzini, F. Pralong and E. Grouzmann, *Cell. Mol. Life Sci.*, 2003, **60**, 350–377.
- 205 M. Körner and J. C. Reubi, *Peptides*, 2007, **28**, 419–425.
- 206 M. Körner, B. Waser and J. C. Reubi, *Lab. Invest.*, 2004, **84**, 71–80.
- 207 M. Körner, B. Waser and J. C. Reubi, *Clin. Cancer Res.*, 2004, **10**, 8426–8433.
- 208 M. Körner, B. Waser and J. C. Reubi, *Int. J. Cancer*, 2005, **115**, 734–741.
- 209 M. Körner, B. Waser and J. C. Reubi, *Clin. Cancer Res.*, 2008, **14**, 5043–5049.
- 210 M. Körner and J. C. Reubi, *J. Neuropathol. Exp. Neurol.*, 2008, **67**, 741–749.
- 211 J. C. Reubi, M. Gugger, B. Waser and J.-C. Schaer, *Cancer Res.*, 2001, **61**, 4636–4641.
- 212 J. C. Reubi, M. Gugger and B. Waser, *Eur. J. Nucl. Med. Mol. Imaging*, 2002, **29**, 855–862.
- 213 M. Langer, R. La Bella, E. Garcia-Garayoa and A. G. Beck-Sickinger, *Bioconjugate Chem.*, 2001, **12**, 1028–1034.
- 214 D. Zwanziger and A. G. Beck-Sickinger, *Curr. Pharm. Des.*, 2008, **14**, 2385–2400.
- 215 D. Zwanziger, I. U. Khan and I. Neundorff, *Bioconjugate Chem.*, 2008, **19**, 1430–1438.
- 216 I. U. Khan, D. Zwanziger, I. Böhme, M. Javed, H. Naseer, S. W. Hyder and A. G. Beck-Sickinger, *Angew. Chem., Int. Ed.*, 2010, **49**, 1155–1158.
- 217 D. Zwanziger, I. Böhme, D. Lindner and A. G. Beck-Sickinger, *J. Pept. Sci.*, 2009, **15**, 856–866.
- 218 P. Antunes, P. D. Raposinho and I. Santos, *Nucl. Med. Biol.*, 2010, **37**, 721.
- 219 B. Guérin, V. Dumulon-Perreault, M. C. Tremblay, S. Ait-Mohand, P. Fournier, C. Dubuc, S. Authier and F. Bénard, *Bioorg. Med. Chem. Lett.*, 2010, **20**, 950–953.
- 220 J. R. Holder and C. Haskell-Luevano, *Med. Res. Rev.*, 2004, **24**, 325–356.
- 221 G. E. Ghanem, G. Comunale, A. Libert, A. Vercammen-Grandjean and F. J. Lejeune, *Int. J. Cancer*, 1988, **41**, 248–255.
- 222 W. Siegrist, F. Solca, S. Stutz, L. Giuffrè, S. Carrel, J. Girard and A. N. Eberle, *Cancer Res.*, 1989, **49**, 6352–6358.
- 223 W. Siegrist, S. Stutz and A. N. Eberle, *Cancer Res.*, 1994, **54**, 2604–2610.
- 224 P. D. Raposinho, J. D. G. Correia, M. C. Oliveira and I. Santos, *Biopolymers*, 2010, **94**, 820–229.
- 225 Y. Miao and T. P. Quinn, *Crit. Rev. Oncol. Hematol.*, 2008, **67**, 213–228.
- 226 J.-Q. Chen, M. F. Giblin, N. Wang, S. S. Jurisson and T. P. Quinn, *Nucl. Med. Biol.*, 1999, **26**, 687–693.
- 227 S. Froidevaux, M. Calame-Christe, H. Tanner, L. Sumanovski and A. N. Eberle, *J. Nucl. Med.*, 2002, **43**, 1699–1702.
- 228 P. D. Raposinho, C. Xavier, J. D. G. Correia, S. Falcão, P. Gomes and I. Santos, *JBIC, J. Biol. Inorg. Chem.*, 2008, **13**, 449–459.
- 229 S. Froidevaux, M. Calame-Christe, J. Shuhmacker, H. Tanner, R. Saffrich, M. Henze and A. N. Eberle, *J. Nucl. Med.*, 2004, **45**, 116–123.
- 230 P. D. Raposinho, J. D. G. Correia, S. Alves, M. F. Botelho, A. C. Santos and I. Santos, *Nucl. Med. Biol.*, 2008, **35**, 91–99.

- 231 Z. Cheng, Z. Xiong, M. Subbarayan, X. Chen and S. S. Gambhir, *Bioconjugate Chem.*, 2007, **18**, 765–772.
- 232 J.-P. Bapst, M. Calame, H. Tanner and A. N. Eberle, *Bioconjugate Chem.*, 2009, **20**, 984–993.
- 233 M. M. Morais, P. D. Raposinho, J. D. G. Correia and I. Santos, *J. Pept. Sci.*, 2010, **16**, 186–186.
- 234 J. P. Bapst, S. Froidevaux, M. Calame, H. Tanner and A. N. Eberle, *J. Recept. Signal Transduction*, 2007, **27**, 383–409.
- 235 J.-Q. Chen, Z. Cheng, N. K. Owen, T. J. Hoffman, Y. Miao, S. S. Jurisson and T. P. Quinn, *J. Nucl. Med.*, 2001, **42**, 1847–1855.
- 236 M. F. Giblin, N. Wang, T. J. Hoffman, S. S. Jurisson and T. P. Quinn, *Proc. Natl. Acad. Sci. U. S. A.*, 1998, **95**, 12814–12818.
- 237 J.-Q. Chen, Z. Cheng, Y. Miao, S. S. Jurisson and T. P. Quinn, *Cancer*, 2002, **94**, 1196–1201.
- 238 Z. Cheng, J. Chen, Y. Miao, N. K. Owen, T. P. Quinn and S. S. Jurisson, *J. Med. Chem.*, 2002, **45**, 3048–3056.
- 239 Y. Miao, K. Benwell and T. P. Quinn, *J. Nucl. Med.*, 2007, **48**, 73–80.
- 240 Y. Miao, N. K. Owen, D. Whitener, F. Gallazzi, T. J. Hoffman and T. P. Quinn, *Int. J. Cancer*, 2002, **101**, 480–487.
- 241 Y. Miao, D. Whitener, W. Feng, N. K. Owen, J. Q. Chen and T. P. Quinn, *Bioconjugate Chem.*, 2003, **14**, 1177–1184.
- 242 Y. Miao, N. K. Owen, R. Darrell, D. R. Fisher, T. J. Hoffman and T. P. Quinn, *J. Nucl. Med.*, 2005, **46**, 121–129.
- 243 P. McQuade, Y. Miao, J. Yoo, T. P. Quinn, M. J. Welch and J. S. Lewis, *J. Med. Chem.*, 2005, **48**, 2985–2992.
- 244 L. Wei, C. Butcher, Y. Miao, F. Gallazzi, T. P. Quinn, M. J. Welch and J. S. Lewis, *J. Nucl. Med.*, 2007, **48**, 64–72.
- 245 L. Wei, Y. Miao, F. Gallazzi, T. P. Quinn, M. J. Welch, A. L. Vavere and J. S. Lewis, *Nucl. Med. Biol.*, 2007, **34**, 945–953.
- 246 M. V. Cantorias, S. D. Figueroa, T. P. Quinn, J. R. Lever, T. J. Hoffman, L. D. Watkinson, T. L. Carmack and C. S. Cutler, *Nucl. Med. Biol.*, 2009, **36**, 505–513.
- 247 Y. Miao, T. J. Hoffman and T. P. Quinn, *Nucl. Med. Biol.*, 2005, **32**, 485–493.
- 248 Y. Miao, T. Shelton and T. P. Quinn, *Cancer Biother. Radiopharm.*, 2007, **22**, 333–341.
- 249 Y. Miao *et al.*, *Clin. Cancer Res.*, 2005, **11**, 5616–5621.
- 250 J. Yang *et al.*, *Bioconjugate Chem.*, 2009, **20**, 1634–1642.
- 251 M. Valldosera, M. Monso, C. Xavier, P. D. Raposinho, J. D. G. Correia, I. Santos and P. Gomes, *Int. J. Pept. Res. Ther.*, 2008, **14**, 273–281.
- 252 J.-Q. Chen, Z. Chen, T. J. Hoffman, S. S. Jurisson and T. P. Quinn, *Cancer Res.*, 2000, **60**, 5649–5658.
- 253 Y. Miao, F. Gallazzi, H. Guo and T. P. Quinn, *Bioconjugate Chem.*, 2008, **19**, 539–547.
- 254 H. Guo, J. Yang, N. Shenoy and Y. Miao, *Bioconjugate Chem.*, 2009, **20**, 2356–2363.
- 255 H. Guo, J. Yang, F. Gallazzi, E. R. Prossnitz, L. A. Sklar and Y. Miao, *Bioconjugate Chem.*, 2009, **20**, 2162–2168.
- 256 H. Guo, J. Yang, F. Gallazzi and Y. Miao, *J. Nucl. Med.*, 2010, **51**, 418–426.
- 257 C. Granier, J. van Rietschoten, P. Kitabgi, C. Poustis and P. Freychet, *Eur. J. Biochem.*, 1982, **124**, 117–124.
- 258 J. C. Reubi, B. Waser, H. Friess, M. Buchler and J. Laissue, *Gut*, 1998, **42**, 546–550.
- 259 J. C. Reubi, B. Waser, J. C. Schaer and J. A. Laissue, *Int. J. Cancer*, 1999, **82**, 213–218.
- 260 G. Pelosi, M. Volante, M. Papotti, A. Sonzogni, M. Masullo and G. Viale, *Q. J. Nucl. Med. Mol. Imaging*, 2006, **50**, 272–287.
- 261 F. Souza, S. Dupouy, V. Viardot-Foucault, E. Bruyneel, S. Attoub, C. Gespach, C. Gompel and P. Forgez, *Cancer Res.*, 2006, **66**, 6243–6249.
- 262 E. Garcia-Garayoa, L. Allemann-Tannahill, P. Blauenstein, M. Willmann, N. Carrel-Remy, D. Tourwe, K. Iterbeke, P. Conrath and P. A. Schubiger, *Nucl. Med. Biol.*, 2001, **28**, 75–84.
- 263 M. Bruehlmeier, E. G. Garayoa, A. Blanc, B. Holzer, S. Gergely, D. Tourwe, P. A. Schubiger and P. Blauenstein, *Nucl. Med. Biol.*, 2002, **29**, 321–327.
- 264 F. Buchegger, F. Bonvin, M. Kosinski, A. O. Schaffland, J. Prior, J. C. Reubi, P. Blauenstein, D. Tourwe, E. Garcia, Garayoa and A. Bischof Delaloye, *J. Nucl. Med.*, 2003, **44**, 1649–1654.
- 265 E. Garcia-Garayoa, P. Blauenstein, A. Blanc, V. Maes, D. Tourwe and P. A. Schubiger, *Eur. J. Nucl. Med. Mol. Imaging*, 2009, **36**, 37–47.
- 266 V. Maes, E. Garcia-Garayoa, P. Blauenstein and D. Tourwe, *J. Med. Chem.*, 2006, **49**, 1833–1836.
- 267 T. Maina, A. Nikolopoulou, E. Stathopoulou, A. S. Galanis, P. Cordopatis and B. A. Nock, *Eur. J. Nucl. Med. Mol. Imaging*, 2007, **34**, 1804–1814.
- 268 E. Garcia-Garayoa, V. Maes, P. Blauenstein, A. Blanc, A. Hohn, D. Tourwe and P. A. Schubiger, *Nucl. Med. Biol.*, 2006, **33**, 495–503.
- 269 M. de Visser, P. J. Janssen, A. Srinivasan, J. C. Reubi, B. Waser, J. L. Erion, M. A. Schmidt, E. P. Krenning and M. de Jong, *Eur. J. Nucl. Med. Mol. Imaging*, 2003, **30**, 1134–1139.
- 270 F. Alshoukr, C. Rosant, V. Maes, J. Abdelhak, O. Raguin, S. Burg, L. Sarda, J. Barbet, D. Tourwe, D. Pelaprat and A. Gruaz-Guyon, *Bioconjugate Chem.*, 2009, **20**, 1602–1610.
- 271 C. J. Smith, W. A. Volkert and T. J. Hoffman, *Nucl. Med. Biol.*, 2005, **32**, 733–740.
- 272 C. Van de Wiele, Filip Dumont, R. V. Broecke, W. Oosterlinck, V. Cocquyt, R. Serreyn, S. Peers, J. Thornback, G. Slegers and R. A. Dierckx, *Eur. J. Nucl. Med. Mol. Imaging*, 2000, **27**, 1694–1699.
- 273 T. J. Hoffman, T. P. Quinn and W. A. Volkert, *Nucl. Med. Biol.*, 2001, **28**, 527–539.
- 274 R. Bella, E. G. Garayoa, M. Bähler, P. Blauenstein, R. Schibli, P. Conrath, D. Tourwe and P. A. Schubiger, *Bioconjugate Chem.*, 2002, **13**, 599–604.
- 275 B. Nock, A. Nikolopoulou, E. Chiotellis, G. Loudos, D. Maintas, J. C. Reubi and T. Maina, *Eur. J. Nucl. Med. Mol. Imaging*, 2003, **30**, 247–258.
- 276 C. J. Smith, G. L. Sieckman, N. K. Owen, D. L. Hayes, D. G. Mazuru, R. Kannan, W. A. Volkert and T. J. Hoffman, *Cancer Res.*, 2003, **63**, 4082–4088.
- 277 K. Lin, A. Luu, K. E. Baidoo, H. H. Gargari, M. K. Chen, K. Brennehan, R. Pili, M. Pomper, M. A. Carducci and H. N. Wagner Jr., *Bioconjugate Chem.*, 2005, **16**, 43–50.
- 278 S. Alves, A. Paulo, J. D. G. Correia, L. Gano, C. J. Smith, T. J. Hoffman and I. Santos, *Bioconjugate Chem.*, 2005, **16**, 438–449.
- 279 B. L. Faintuch, R. L. S. R. Santos, A. L. F. M. Souza, T. J. Hoffman, M. Greeley and C. J. Smith, *Synth. React. Inorg., Met.-Org., Nano-Met. Chem.*, 2005, **35**, 43–51.
- 280 B. A. Nock, A. Nikolopoulou, A. Galanis, P. Cordopatis, B. Waser, J. C. Reubi and T. Maina, *J. Med. Chem.*, 2005, **48**, 100–110.
- 281 S. Alves, J. D. G. Correia, I. Santos, B. Veerendra, G. L. Sieckman, T. J. Hoffman, T. L. Rold, S. D. Figueroa, L. Retzlaff, J. McCrate, A. Prasanphanich and C. J. Smith, *Nucl. Med. Biol.*, 2006, **33**, 625–634.
- 282 N. Agorastos, L. Borsig, A. Renard, P. Antoni, G. Viola, B. Spingler, P. Kunz and R. Alberto, *Chem.–Eur. J.*, 2007, **13**, 3842–3852.
- 283 E. G. Garayoa, D. Rüegg, P. Blauenstein, M. Zwimpfer, I. U. Khan, V. Maes, A. Blanc, A. G. B. Sicking, D. A. Tourwe and P. A. Schubiger, *Nucl. Med. Biol.*, 2007, **34**, 17–28.
- 284 F. Prasanphanich, S. R. Lane, S. D. Figueroa, L. Ma, T. L. Rold, G. L. Sieckman, T. J. Hoffman, J. M. McCrate and C. J. Smith, *In Vivo*, 2007, **21**, 1–16.
- 285 J. U. Kunstler, B. Veerendra, S. D. Figueroa, G. L. Sieckman, T. L. Rold, T. J. Hoffman, C. J. Smith and H. J. Pietzsch, *Bioconjugate Chem.*, 2007, **18**, 1651–1661.
- 286 S. L. Lane, B. Veerendra, T. L. Rold, G. L. Sieckman, T. J. Hoffman, S. S. Jurisson and C. J. Smith, *Nucl. Med. Biol.*, 2008, **35**, 263–272.
- 287 R. Cescato, T. Maina, B. Nock, A. Nikolopoulou, D. Charalambidis, V. Piccand and J. C. Reubi, *J. Nucl. Med.*, 2008, **49**, 318–326.
- 288 J. Shi, B. Jia, Z. Liu, Z. Yang, Z. Yu, K. Chen, X. Chen, S. Liu and F. Wang, *Bioconjugate Chem.*, 2008, **19**, 1170–1178.
- 289 E. A. Fragogeorgi, C. Zikos, E. Gourni, P. Bouziotis, M. P. Petsotas, G. Loudos, N. Mitsokapas, S. Xanthopoulos, M. M. Vavayanni, E. Livanou, A. D. Varvarigou and S. C. Archimandritis, *Bioconjugate Chem.*, 2009, **20**, 856–867.
- 290 K. Abiraj, R. Mansi, M. L. Tamma, F. Forren, R. Cescato, J. C. Reubi, K. G. Akyel and H. R. Maecke, *Chem.–Eur. J.*, 2010, **16**, 2115–2124.
- 291 B. E. Rogers, H. M. Bigott, D. W. McCarthy, D. Della Manna, J. Kim, T. L. Sharp and M. J. Welch, *Bioconjugate Chem.*, 2003, **14**, 756–763.
- 292 X. Chen, R. Park, Y. Hou, M. Tohme, A. H. Shahinian, J. R. Bading and P. S. Conti, *J. Nucl. Med.*, 2004, **45**, 1390–1397.
- 293 B. E. Rogers, D. D. Maina and A. Safavy, *Cancer Biother. Radiopharm.*, 2004, **19**, 25–34.
- 294 Y. S. Yang, X. Zhang, Z. Xiong and X. Chen, *Nucl. Med. Biol.*, 2006, **33**, 371–380.
- 295 J. J. Parry, T. S. Kelly, R. Andrews and B. E. Rogers, *Bioconjugate Chem.*, 2007, **18**, 1110–1117.
- 296 G. B. Biddlecombe, B. E. Rogers, M. de Visser, J. J. Parry, M. de Jong, J. L. Erion and J. S. Lewis, *Bioconjugate Chem.*, 2007, **18**, 724–730.

- 297 J. C. Garrison, T. L. Rold, G. L. Sieckman, S. D. Figueroa, W. A. Volkert, S. S. Jurisson and T. J. Hoffman, *J. Nucl. Med.*, 2007, **48**, 1327–1337.
- 298 A. F. Prasanphanich, P. K. Nanda, T. L. Rold, L. Ma, M. R. Lewis, J. C. Garrison, T. J. Hoffman, G. L. Sieckman, S. D. Figueroa and C. J. Smith, *Proc. Natl. Acad. Sci. U. S. A.*, 2007, **104**, 12462–12467.
- 299 A. F. Prasanphanich, L. Retzliff, S. R. Lane, P. K. Nanda, G. L. Sieckman, T. L. Rold, L. Ma, S. D. Figueroa, S. V. Sublett, T. J. Hoffman and C. J. Smith, *Nucl. Med. Biol.*, 2009, **36**, 171–181.
- 300 S. R. Lane, P. Nanda, T. L. Rold, G. L. Sieckman, S. D. Figueroa, T. J. Hoffman, S. S. Jurisson and C. J. Smith, *Nucl. Med. Biol.*, 2010, **37**, 751–761.
- 301 M. Hofmann, S. Machtens, C. Stief, F. Länger, A. R. Boerner, H. Maecke and W. H. Knapp, *Eur. J. Nucl. Med. Mol. Imaging*, 2004, **31**, S253.
- 302 A. Dimitrakopoulou-Strauss, P. Hohenberger, U. Haberkorn, H. R. Macke, M. Eisenhut and L. G. Strauss, *J. Nucl. Med.*, 2007, **48**, 1245–1250.
- 303 H. Zhang, J. Schuhmacher, B. Waser, D. Wild, M. Eisenhut, J. C. Reubi and H. R. Maecke, *Eur. J. Nucl. Med. Mol. Imaging*, 2007, **34**, 1198–1208.
- 304 T. J. Hoffman, H. Gali, C. J. Smith, G. L. Sieckman, D. L. Hayes, N. K. Owen and W. A. Volkert, *J. Nucl. Med.*, 2003, **44**, 823–831.
- 305 T. Maina, B. A. Nock, H. Zhang, A. Nikolopoulou, B. Waser, J. C. Reubi and H. R. Maecke, *J. Nucl. Med.*, 2005, **46**, 823–830.
- 306 M. de Visser, H. F. Bernard, J. L. Erion, M. A. Schmidt, A. Srinivasan, B. Waser, J. C. Reubi, E. P. Krenning and M. de Jong, *Eur. J. Nucl. Med. Mol. Imaging*, 2007, **34**, 1228–1238.
- 307 C. L. Ho, L. C. Chen, W. C. Lee, S. P. Chiu, W. C. Hsu, Y. H. Wu, C. H. Yeh, M. G. Stabin, M. L. Jan, W. J. Lin, T. W. Lee and C. H. Chang, *Cancer Biother. Radiopharm.*, 2009, **24**, 435–443.
- 308 C. J. Smith, H. Gali, G. L. Sieckman, D. L. Hayes, N. K. Owen, D. G. Mazuru, W. A. Volkert and T. J. Hoffman, *Nucl. Med. Biol.*, 2003, **30**, 101–109.
- 309 H. Zhang, J. Chen, C. Waldherr, K. Hinni, B. Waser, J. C. Reubi and H. R. Maecke, *Cancer Res.*, 2004, **64**, 6707–6715.
- 310 C. V. Johnson, T. Shelton, C. J. Smith, L. Ma, M. C. Perry, W. A. Volkert and T. J. Hoffman, *Cancer Biother. Radiopharm.*, 2006, **21**, 155–166.
- 311 L. E. Lantry, E. Cappelletti, M. E. Maddalena, J. S. Fox, W. Feng, J. Chen, R. Thomas, S. M. Eaton, N. J. Bogdan, T. Arunachalam, J. C. Reubi, N. Raju, E. C. Metcalfe, L. Lattuada, K. E. Linder, R. E. Swenson, M. F. Tweedle and A. D. Nunn, *J. Nucl. Med.*, 2006, **47**, 1144–1152.
- 312 B. Waser, V. Eltschinger, K. Linder, A. Nunn and J. C. Reubi, *Eur. J. Nucl. Med. Mol. Imaging*, 2007, **34**, 95–100.
- 313 M. E. Maddalena, J. Fox, J. Chen, W. Feng, A. Cagnolini, K. E. Linder, M. F. Tweedle, A. D. Nunn and L. E. Lantry, *J. Nucl. Med.*, 2009, **50**, 2017–2024.
- 314 R. Thomas, J. Chen, M. M. Roudier, R. L. Vessella, L. E. Lantry and A. D. Nunn, *Clin. Exp. Metastasis*, 2009, **26**, 105–119.